Article

Not peer-reviewed version

Mathematical Model of Tapered Thread Profile Made by Turning from Different Machinability Materials

Oleh Onysko *, Volodymyr Kopei, Cristian Barz, Yaroslav Kusyi, Saulius Baskutis, Michal Bembenek, Predrag Dašić, Vitalii Panchuk

Posted Date: 12 March 2024

doi: 10.20944/preprints202403.0719.v1

Keywords: cutting edge inclination angle; lathe tool rake angle; lead screw angle; convolute helicoid; oblique helicoid; generator of ruled helicoid

Article

Mathematical Model of Tapered Thread Profile Made by Turning from Different Machinability Materials

Oleh Onysko [1,*], Volodymyr Kopei [1,2], Cristian Barz [3], Jaroslav Kusyi [4], Saulius Baskutis [5], Michal Bembenek [6], Predrag Dašić [7] and Vitalii Panchuk [1,8]

[1] Department of Computerized Mechanical Engineering, Ivano-Frankivsk National Technical University of Oil and Gas, Karpatska str., no. 15, 76019 Ivano-Frankivsk, Ukraine
[2] volodymyr.kopey@nung.edu.ua
[3] North University Centre of Baia Mare, Technical University of Cluj-Napoca, Victor Babes str., no.62A.,430083 Baia Mare, Romania; cristian.barz@ieec.utcluj.ro
[4] Lviv Polytechnic National University, Department of Mechanical Engineering and Transport, Stepan Bandera str., no. 12, 79013 Lviv, Ukraine; jarkym@ukr.net
[5] Kaunas University of Technology, Department of Production Engineering, 56, Studentu St., Kaunas 51424, Lithuania; saulius.baskutis@ktu.lt
[6] AGH University of Science and Technology in Kraków, Department of Mechanical Engineering and Robotics, 30 Mickiewicza Avenue 30-059 Krakow, Poland; bembenek@agh.edu.pl
[7] SaTCIP Publisher Ltd., Street Tržni Centar Pijaca 101, 36210 Vrnjačka Banja, Serbia; dasicp58@gmail.com
[8] vitalii.panchuk@nung.edu.ua
* Correspondence: oleh.onysko@nung.edu.ua

Abstract: High-precision conical threads are widely used in responsible joints in the drilling of oil and gas wells. Difficult underground drilling conditions due to the occurrence of significant mechanical loads and an aggressive environment in wells require the use of workable materials that are often difficult to machine. The huge need for such connections dictates the use of high-performance cutting tools, which means that high demands are placed on their effective geometric performance. The study describes the theoretical dependence of the profile precision of the tapered drill-string tool-joint threads of all standard sizes on the complex of a cutting tool geometric parameters and cutting tool setting accuracy. The experiments include an assessment of the geometric accuracy of the profile of the obtained NC23 thread connector, depending on the values of the installation angles and the declared tangential displacement of the standard threaded carbide insert.

Keywords: cutting edge inclination angle; lathe tool rake angle; lead screw angle; convolute helicoid; oblique helicoid; generator of ruled helicoid

1. Introduction

Today, oil and gas extraction, and in particular drilling, is a key process for a number of applied industries that play a strategic role in guaranteeing economic stability. In particular, this is exploration and extraction of hydrocarbons, geothermal and mineral resources; environmental monitoring and scientific research of the subsoil; underground archaeological excavations and infrastructure development of large cities, etc. [1–4]. Drilling and casing strings and pipelines are complex, of great length, elastic mechanical systems made of metallic and non-metallic materials, with a large number of threaded connections [5–7], which interact with the rock [8].

Threaded connections are used to maintain the structural integrity and tightness of pipe columns in wells and pipelines, so the quality of their materials [9, 10] and the reliability of the structure are subject to increased requirements [11–13]. A key advantage of threaded connections compared to other methods of connecting pipes and tools in the drill string is that they can be disassembled and reused many times. At the same time, this advantage can become a source of problems for the entire structure due to unintentional self-unscrewing of the threaded connection [14–16]. This phenomenon

Preprints.org (www.preprints.org) | NOT PEER-REVIEWED | Posted: 12 March 2024 doi:10.20944/preprints202403.0719.v1

can lead to significant financial losses in the industry due to the need for regular maintenance of connections, as well as cause emergency situations [17].

In most cases, threaded connections for drill string elements work in aggressive and abrasive environments under the influence of intense dynamic and long-term cyclic loads [18, 19]. The increase in drilling depths and the construction of wells with a complex spatial configuration require the use of modern materials, intelligent structures and advanced technologies for designing and manufacturing drill tool joints [20–23]. The stress state of pipes and cylindrical shells near sharp-end concentrators under the conditions of contact interaction was studied in papers [24–29].

Operating experience shows that most problems and destruction of threaded connections can be eliminated by improving the perfection of their design [30–32], a smaller part of failures is caused by technological aspects [33] and operational errors [34, 35].

The technology of manufacturing helical and toothed surfaces requires an analytical approach to their shaping [36], optimization of the technological route [37, 38], study of the latest approaches to stabilization of turning processes [39] and development of special designs of cutting tools to ensure their shaping with minimal errors [40, 41]. Optimization of high-performance cutting modes in the manufacture of threads requires an analysis of the tools wear and the nature of changes in the roughness and accuracy of the thread, as well as the development of new methods of thread formation [42].

The purpose of this study is to establish a model for ensuring the accuracy of forming a thread with a given triangular or trapezoidal profile, functionally depending on its pitch, diameter and geometric parameters of the turning tool that performs it, using an analytical method.

Chapter 1 of the paper shows the relevance of the research; chapter 2 describes the modern theoretical provisions on ensuring the accuracy of thread manufacturing; chapter 3 presents the proof of the mathematical model of a tapered thread profile as a function of the geometric parameters of the cutter which performed it; chapter 4 shows the results of the research obtained using the algorithm, which was created on the basis of the mathematical model; chapter 5 presents the conclusions of study.

2. Modern Approaches to Ensuring the Accuracy of the Production of Large-Step Drill Pipe Tapered Threads

Drill pipe joints (also known as tool-joints) are large-pitch threaded male-female conical joints (nipple-coupling) with a diameter of 30 to 200 mm and of a triangular profile (Figure 1).

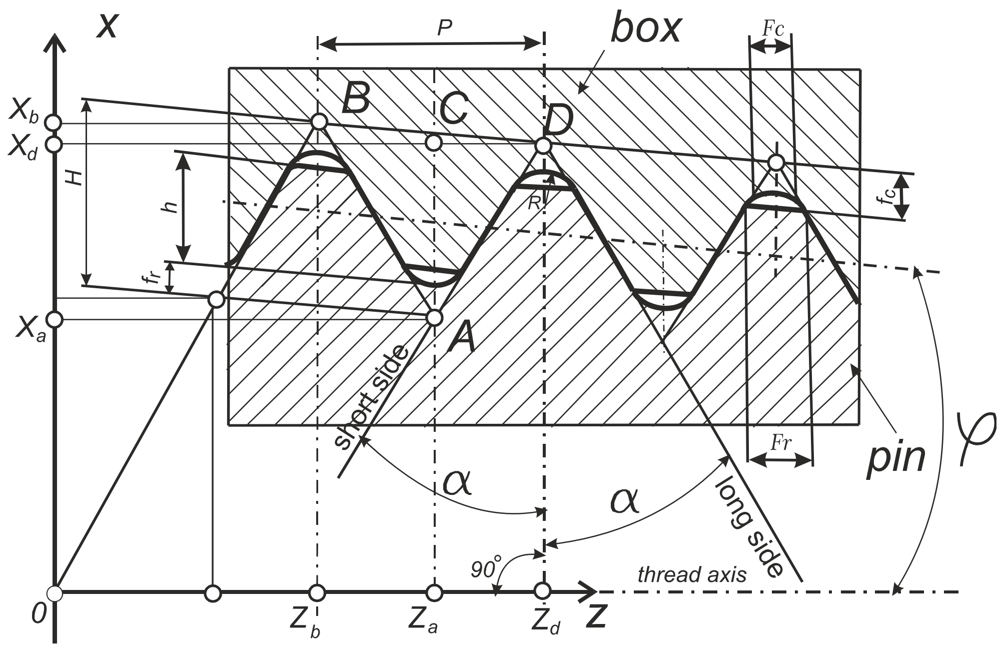

 doi:10.20944/preprints202403.0719.v1

Figure 1. Scheme of a drill-string threaded connection according to the API7 standard with reference to the *ZOX* rectangular coordinate system. *H* - thread height (not truncated), *h* - thread height (truncated), *fr* - root truncation, *fc* - crest truncation, *R* - root radius, *P* - pitch.

One of the requirements for the accuracy of the drill-string tool-joint thread is the accuracy of its half-profile angle α, which according to the standard [43] is the same for all its standard sizes and is 30°±0.75° (Figure 1). Drill-string thread connectors are made using lathes, and thread cutters are used to turn their threaded surfaces. Modern manufacturers recommend using cutting tools with a full profile, which is similar to the profile and pitch *P* of one of the standard sizes of threading the tool-joint [44]. At the same time, tool manufacturers offer a variety of materials and coatings for cutting inserts, recommend different tool feeding schemes to achieve better productivity or stability of the cutter. In scientific works [45-46], methods of cutting in the process of thread turning from hard-to-machine AISI 304L stainless steels are investigated for aim to reach a high stability of the cutter. At the same time, the geometry of the rake surface of the cutter is never regulated by manufacturers, that is, their rake angle is actually always equal to 0. Despite the established approach of manufacturers, there are scientific studies that indicate the feasibility of using a non-zero value of the rake angle γ for turning in general and for turning oil and gas conical threads, in particular, threads made of high-alloy steel with a content of 13% Cr [47-48] (Figure 2).

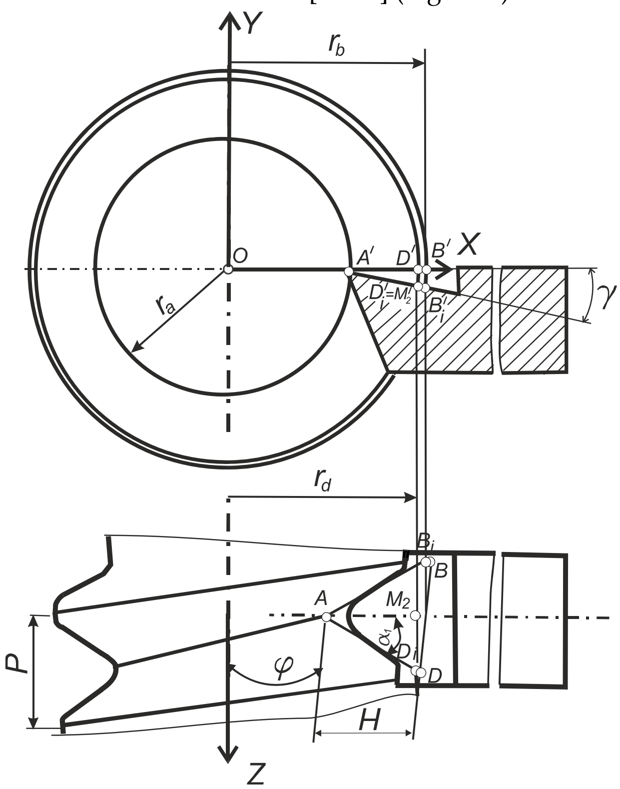

Figure 2. Scheme of installing a threaded cutter with a non-zero value of the rake angle (γ>0).

The zero-value rake angle of the cutters offered by the manufacturers is obviously related to compliance with the precision of the drill-string tool-joint thread regulated by the standard [43]. Theoretical studies of the kinematics of the process of turning tapered thread using a tool with a non-zero value of the rake angle are presented in studies [49–50]. However, the scientific results in these works concern the analytical calculations of the accuracy of the kinematics of turning the thread [49] and its predicted lead angle [50], and not its profile. Experimental studies of the influence of the error of setting the threaded cutter on the deviation of the real profile of the thread were carried out in [51]. The input data in this study are the tangential deviation of the cutter installation relative to the axis of the thread, as well as the angular displacement relative to the longitudinal axis of the tool. An analytical study of the effect of tool kinematics on the profile of the screw was carried out by the authors [52], but the object of the study is a cylindrical worm screw, and the subject is the profile and

Preprints.org (www.preprints.org) | NOT PEER-REVIEWED | Posted: 12 March 2024 doi:10.20944/preprints202403.0719.v1

kinematics of the end mill, not the geometric angular parameters of its cutting edge. The work [53] contains analytical dependences of the tool profile depending on its rake angle, but the tool is intended for the manufacture of a roller-gear cam and not a conventional worm (screw) shaft.

In cutters with a non-zero rake angle, the rectilinear section of the cutting edge of the tool does not cross the axis of the thread (Figure 2). In this case, as a result of the helical movement of the straight L, that is, the straight *AD* where the straight section of the cutting edge is located, a surface topology other than that prescribed by the standard is formed, i.e. instead of the Archimedean helicoid (Figure 3), a convoluted helicoid (Figure 4) is formed.

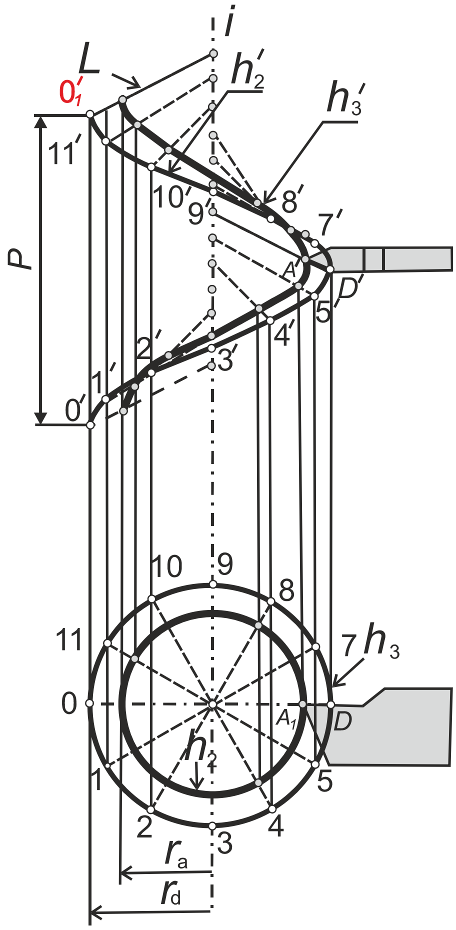

Figure 3. Scheme of execution of an oblique closed helicoid using a lathe cutter.

As it is known, helices are the guides of screws, so the drawings in Figure 3 and Figure 4 show the inner helix h_2, on which the points of the inner radius of the thread r_a are theoretically located, and the outer helix h_3, on which the points of the outer radius of the thread r_d are theoretically located. The axis of screws *i* corresponds to the thread axis *Z* in Figure 2.

Additional characteristics for a convolute screw are as follows: an output cylinder with a radius r_1 and a helix h_1 on it (Figure 4).

Preprints.org (www.preprints.org) | NOT PEER-REVIEWED | Posted: 12 March 2024 doi:10.20944/preprints202403.0719.v1

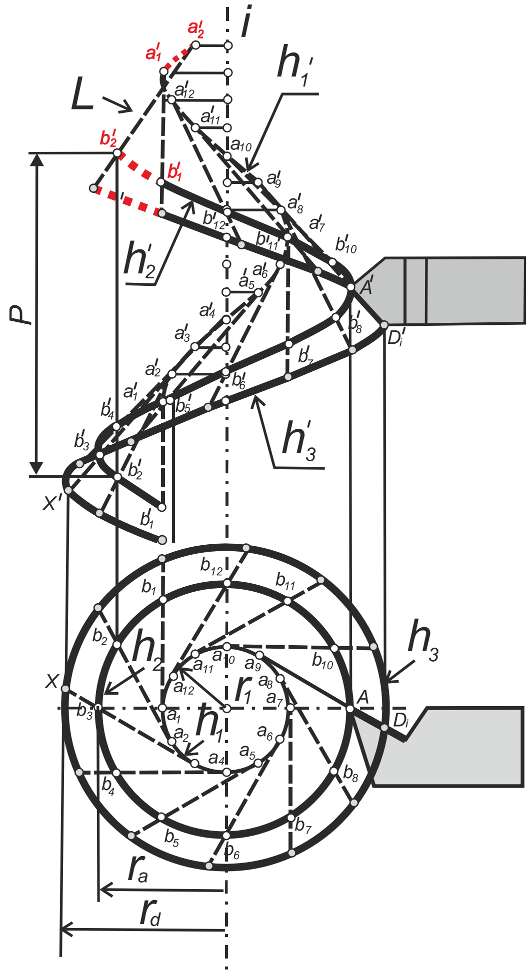

Figure 4. Scheme of execution of a convolute helicoid using a lathe cutter.

Analogous constructions apply to and can be performed for another perpendicular section of the cut, located on the line *AB*, which is shown in Figure 2.

Based on the data of the draftsman of the standard [43], the starting point for designing the profile of the cutter is the Archimedean spiral surface, since the left *AD* and right *AB* of its lateral sides of its profile are rectilinear and such a cut is called triangular. Therefore, the axial profile of this surface is described by the equation of an algebraic linear function (Figure 1)

$$z = tan(\alpha)x, \quad (1)$$

where the angle $\alpha = 30°$ is the half-profile angle of the triangular thread.

To determine the theoretical profile of a cut formed by a cutter, the cutting edge of which does not lie in its axial section, it is necessary to have an analytical dependence of the axial section of the convolute helicoid on the value of the rake angle γ at the tool nose and the thread diameter, and to carry out its analytical comparison with the profile formula of the given thread (1).

Since the thread is conical, the variable nature of the values r_a, r_b, r_1 should be taken into account in the calculations:

$$\begin{aligned} r_a &= r_{amin} \cdot l \cdot cos(\varphi), \\ r_b &= r_{bmin} \cdot l \cdot cos(\varphi), \quad (2) \\ r_1 &= r_{1min} \cdot l \cdot cos(\varphi), \end{aligned}$$

where r_{amin}, r_{bmin}, r_{1min} are minimum values of radii r_a, r_b, r_1; l is the distance from the beginning of the screw thread with the small cone base to a certain turn of it.

Preprints.org (www.preprints.org) | NOT PEER-REVIEWED | Posted: 12 March 2024 doi:10.20944/preprints202403.0719.v1

2.1. Methodology of the Study of the Effect of the Value of the Back Rake Angle of the Lathe Cutter Nose on the Profile of Tapered Thread Obtained with Using it

In Figure 5, the generator L of the convoluted helicoid is constructed in cylindrical coordinates and at the same time in Cartesian coordinates. The XY plane is perpendicular to the Z axis, which coincides with the thread axis and contains the starting point of coordinates O. Cylindrical coordinates are the most suitable for modelling the process of forming a helical surface with a turning tool.

The generator L of the convolute screw intersects the X axis at point A, and it is inclined to the $X0Y$ plane at an angle α_1 (Figure 5). In the case of using a conventional cutting tool, the profile angles of the thread and the cutter are identical, i.e. $\alpha_1 = \alpha$. The projection of the generating L onto the coordinate plane $X0Y$ is the straight line M_1M_2. The segment AD_i lies on the generating L and it is the cutting edge of the cutter. The plane defined by the triangle AD_iM_2 is the rake plane of the thread lathe tool. At the same time, the segment AD_iM_2 is parallel to the Z axis, and its length is $|D_iM_2|$ determines the Z coordinate of point D. The segment AM_2 is the projection of the cutting edge AD_i on the $X0Y$ plane. Point M_1 is the point of contact of the straight M_1M_2 to the initial cylinder with radius r_1 [54].

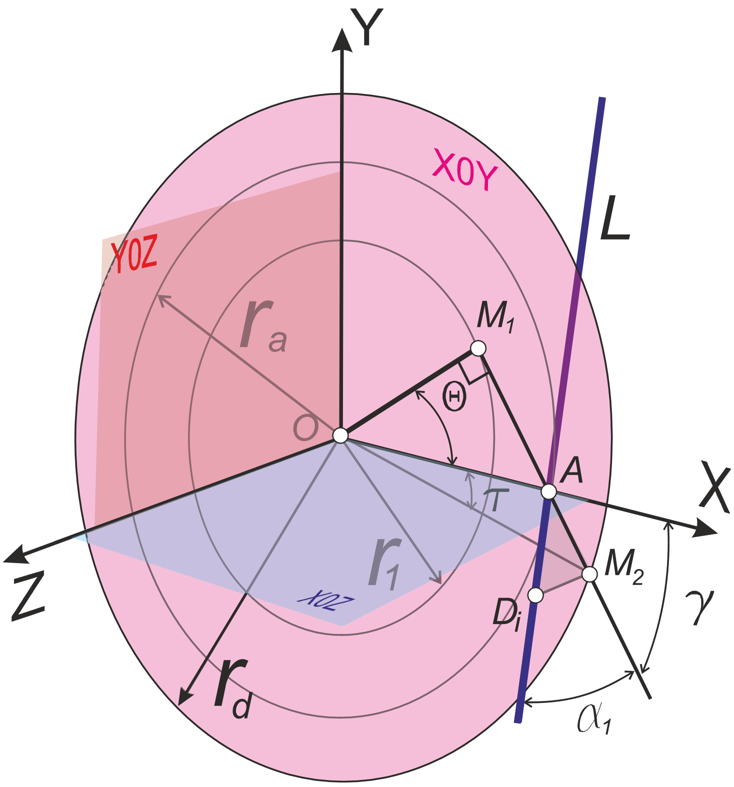

Figure 5. Schematic of placement of the rake surface of the thread cutter in cylindrical coordinates.

2.1.1. Parametric Equations of the Helical Surface and Equations of Its Axial Section in General Form

If the generatrix L is set by a system of equations in cylindrical coordinates:

$$\begin{cases} \rho = f(\tau), \\ Z = F(\tau), \end{cases} \tag{3}$$

where the projection of L onto the $X0Y$ plane (line M_1M_2) is defined in polar coordinates by the equation:

$$\rho = f(\tau), \tag{4}$$

where ρ is the distance of an arbitrary point of segment AM_2 to point O, then the helical surface is written in a follow system of equations:

Preprints.org (www.preprints.org) | NOT PEER-REVIEWED | Posted: 12 March 2024 doi:10.20944/preprints202403.0719.v1

$$\begin{cases} X = f(\tau)\, cos(\tau + \theta)\,, \\ Y = f(\tau)\, sin(\tau + \theta), \\ Z = F(\tau) + p\theta, \end{cases} \tag{5}$$

where:

— parameters τ and θ determine the position of a point on the surface and are its curvilinear coordinates. At the same time, the parameter τ determines the position of an arbitrary point of the line M_1M_2 on the projection of the generating line L on the $X0Y$ plane. The parameter θ determines the amount of rotation of the generator L around the Z axis;

— the value p is a parameter of the screw and is determined by the formula

$$p=P2\pi,$$

where P is the pitch of helicoid.

If we solve equation (4) with respect to the parameter τ:

$$\tau = f_1(\rho), \tag{6}$$

then the system of equations (3) of the generatrix L in cylindrical coordinates will take the following form:

$$\begin{cases} \tau = f_1(\rho), \\ z = F_1(\rho), \end{cases} \tag{7}$$

where $F_1(\rho)$ denotes a certain complex function:

$$F\big(f_1(\rho)\big) = F_1(\rho).$$

Thus, the system of equations (5) of the helical surface will have the following form:

$$\begin{cases} X = \rho\, cos(\tau + \theta)\,, \\ Y = \rho\, sin(\tau + \theta)\,, \\ Z = F_1(\rho) + p\theta, \end{cases} \tag{8}$$

where the parameter τ must be replaced by formula (6). The coordinate lines are: at θ=*const* is the generating line L, and at τ=*const* is the spiral line, which is placed on a cylinder with a radius of ρ.

Let's bring the system of equations (8) to new curvilinear coordinates by making a substitution:

$$\varphi = \tau + \Theta.$$

The system of equations of the helical surface (8) will take the following form:

$$\begin{cases} X = \rho\, cos(\varphi)\,, \\ Y = \rho\, sin(\varphi)\,, \\ Z = F(\rho) + p\varphi, \end{cases} \tag{9}$$

where:

$$F(\rho) = F_1(\rho) - p\tau.$$

Here (ρ, φ) are the curvilinear coordinates of a point on a helical surface, if φ=*const*, then we have the generating L, and if ρ=*const*, then we have a helical line. The function $F(\rho)$ determines the law of change of the Z coordinate of the current point of the guide L and it can be written as follows:

$$F(\rho) = F\ \ (\tau) - p\tau = z - p\tau. \tag{10}$$

The geometric content of the function (10) is easy to find if we substitute φ=0.
into the system of equations (9). Then we will get the following equation system in parametric form:

$$\begin{cases} X = \rho, \\ Y = 0, \\ Z = F(\rho), \end{cases}$$

or, which is the same after removing the parameter ρ:

Preprints.org (www.preprints.org) | NOT PEER-REVIEWED | Posted: 12 March 2024 doi:10.20944/preprints202403.0719.v1

$$\begin{cases} Y = 0, \\ Z = F(x). \end{cases} \quad (11)$$

The system of equations (11) determines the line of intersection of the helical surface with the $X0Z$ plane, i.e., they analytically describe the axial section of the convolute helical surface.

2.1.2. The Influence of the Back Rake Angle at the Nose of Lathe Tool on the Profile of the Helical Convoluted Surface Obtained with Help of it

Looking at the triangle OM_1M_2 (Figure 6), we can determine the value of the radius of the main cylinder r_1:

$$r_1 = r_a\, cos(\theta) = r_a\, cos\left(\frac{\pi}{2} - \gamma\right) = r_a\, sin\,\gamma. \quad (12)$$

Since the axis OX is taken as the polar axis, the polar coordinates (ρ, τ) will determine the position of the segment AM_2, which is the projection of the cutting-edge AD on the $X0Y$ plane.

Let the point M_2 be one of the arbitrary points of the segment AM_2, then the curvilinear coordinate ρ will be the segment of variable value $|OM_2|$. Using the triangle OM_1M_2 and using formula (12), we find the variable value ρ:

$$\rho(\tau) = \frac{r_a\, sin\,\gamma}{cos\left(\tau + \frac{\pi}{2} - \gamma\right)} = \frac{r_a\, sin\,\gamma}{sin(\gamma - \tau)}. \quad (13)$$

The obtained expression (13) corresponds to formula (4), that is, the first of the equations system (3) of the cutting edge AD_i in cylindrical coordinates.

Using the theorem of sines, we find the value of the segment OAM_2 from the triangle (AM_2):

$$|AM_2| = \frac{r_a\, sin\,\tau}{sin(\gamma - \tau)}.$$

From the right-angled triangle AD_iM_2, we can obtain the value of the segment length (D_iM_2):

$$|D_iM_2| = tan(\alpha_1)|AM_2| = tan(\alpha_1)\frac{r_a\, sin\,\tau}{sin(\gamma - \tau)}.$$

Since the point M_2 is accepted by us as arbitrary, it can be assumed that the length of the segment D_iM_2 is a variable value and corresponds to 3-coordinate of an arbitrary point of the cutting edge AD_i in cylindrical coordinates. So instead of $|D_iM_2|$ we substitute $Z(\tau)$:

$$Z(\tau) = tan(\alpha_1)\frac{r_a\, sin\,\tau}{sin(\gamma - \tau)}. \quad (14)$$

The obtained equation (14) corresponds to other of the system of equations (3), which describes the generatrix L in cylindrical coordinates.

According to formula (6) and using formula (13), we solve that equation with respect to τ:

$$\tau = \gamma - arcsin\left(\frac{r_a\, sin\,\gamma}{\rho}\right). \quad (15)$$

The next step according to formula (7) should be the solution of Z coordinate with respect to ρ, that is, formula (15) should be substituted into equation (14). Therefor we get the following dependence:

$$z(\rho) = tan(\alpha_1)\frac{r_a\, sin\left(\gamma - arcsin\left(\frac{r_a\, sin\,\gamma}{\rho}\right)\right)}{sin\left(\gamma - \left(\gamma - arcsin\left(\frac{r_a\, sin\,\gamma}{\rho}\right)\right)\right)}.$$

After some reductions, the resulting equation will take the following form:

$$z(\rho) = tan(\alpha_1)\rho\frac{sin\left(\gamma - arcsin\left(\frac{r_a\, sin\,\gamma}{\rho}\right)\right)}{sin\,\gamma}. \quad (16)$$

Preprints.org (www.preprints.org) | NOT PEER-REVIEWED | Posted: 12 March 2024 doi:10.20944/preprints202403.0719.v1

To obtain the system of equations of the helical surface according to formulas (9), the function (16) should be transformed according to formula (10) and as a result, according to formula (11), the equation of the axial section of the convoluted helical surface should be obtained [52]:

$$Z(x) = tan(\alpha_1)x\frac{\sin\tau}{\sin\gamma} - \frac{P}{2\pi}\tau, \quad (17)$$

where:

τ is one of the curvilinear coordinates of the cutting edge, determined by the formula:

$$\tau = \gamma - arcsin\left(\frac{r_a \sin\gamma}{x}\right);$$

P is the pitch of the specified thread;

γ is the rake angle;

α_1 is the half-profile angle of the cutting edge in the rake plane.

The received transcendental equation (17) of the axial profile of the convolute helical cut made by the cutter indicates its theoretical discrepancy with the profile of the Archimedean thread given by the standard, which is described by the algebraic equation of the first order (1).

However, τ=0, $\frac{\sin\tau}{\sin\gamma} = 1$, and $\frac{P}{2\pi}\tau = 0$, if the angle γ approaches 0, and then equation (17) becomes equivalent to equation (1).

The authors in the study [55], due to the algorithm developed by the authors, concluded that it is admissible to use threaded cutters with a back rake angle of γ=12° for the manufacture of a tool-joint thread 2 7/8 Reg. At the same time, the deviation from the nominal half-profile angle is less than 0.1°, which is less than 15% of the tolerance. In the article [48], the authors proposed a scheme for ensuring a negative rake angle due to a simple geometric change of the holder of a conventional thread cutter (Figure 6). With such a change, there is no need to create a new cutting insert or a method of its attachment at a certain back rake angle γ.

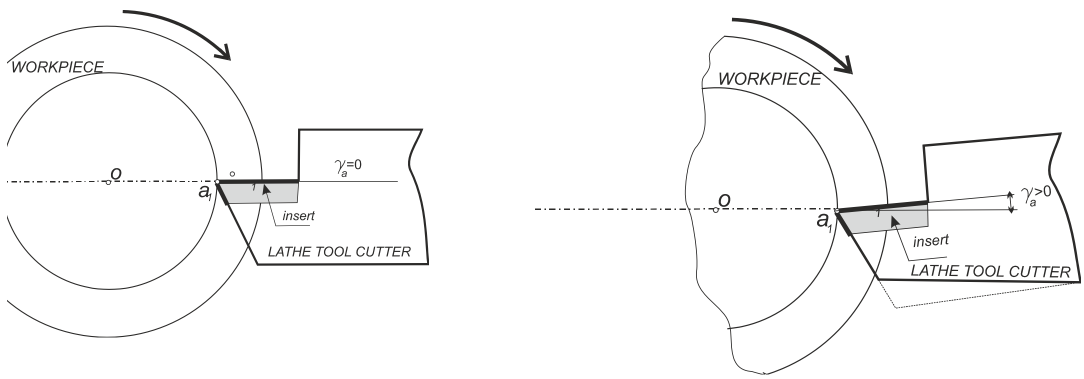

(a) (b)

Figure 6. The scheme of ensuring the specified value of the back rake angle γ: (**a**) Conventional tool with back rake angle γ=0; (**b**) Modernized tool shank with a changed tool-base with back rake angle γ<0.

2.1.3. The Influence of the Inclination Angle of the Cutting Edge of the Thread Cutter on the Profile of the Helical Convolute Surface Obtained with it

In fact, the surface of the convoluted helicoid is also obtained due to the inclination of the cutting insert at an angle λ relative to the axis of the thread, which is recommended to improve the operating conditions of the cutter (Figure 7). The angle λ is chosen so that it corresponds to the rang between the angle of inclination of the screw on the depressions ψ_{BH} and on the protrusion ψ_3 ($\psi_{BH} < \lambda < \psi_3$).

Preprints.org (www.preprints.org) | NOT PEER-REVIEWED | Posted: 12 March 2024 doi:10.20944/preprints202403.0719.v1

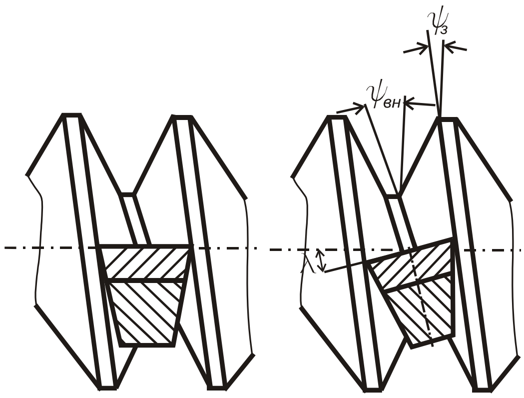

Figure 7. Scheme of installing the cutter perpendicular to the inclination of the screw turn: on the left – without the inclination of the cutting insert ($\lambda = 0$), on the right – with the inclination of the cutting insert ($\lambda > 0$).

Such an angle for tool-joints is quite insignificant, it does not cause alarm among manufacturers regarding the influence on the accuracy of the thread profile, and therefore the operating instructions for threaded cutters contain the method of using tools containing a plate installed at an angle relative to the axis of the thread. However, for large-pitch screw surfaces, including conical ones, the influence of the angle of inclination of the tool on the accuracy of their axial cross-section, that is, the thread profile, turns out to be quite significant [22, 56]. The study proves that for high-precision worm drives, reducing the backlash with a high degree is quite a difficult task. This work is based on the analysis of the accuracy of the kinematics of manufacturing convolute and involute worm screws, but does not focus on the geometric parameters of the tools for their manufacture. In the study [57], the authors Onysko and Kopei prove by calculations that the presence of a screw lead angle of λ = 2.24° for the NC10 tool-joint thread (the smallest size among drill-string connect thread), and accordingly, the angle of inclination of the cutting edge of the cutter λ_z=2.24° causes a decrease of the half-profile angle $\alpha/2$ by 0.24°, which is more than 30% of the tolerance. The methodology of the theoretical part of that research is essentially a continuation of the approaches presented in Figure 5 and described by equation (17).

In Figure 8 presents a scheme for compiling an algorithm for calculating the deviation of the received profile of the convolute surface from the profile of the thread specified by the standard, depending on the angle of inclination of the cutting edge of the thread cutter λ_z. The scheme is built in cylindrical coordinates. The Z axis of the coordinate system coincides with the axis of the screw. The value r_1 denotes the radius of the main cylinder on which the guide helix of the convolute screw is placed, and r_a and r_d correspond to the scheme of the conical cut in Figure 2. The $X0Y$ plane is perpendicular to the Z axis and contains the point of origin of coordinates O.

 doi:10.20944/preprints202403.0719.v1

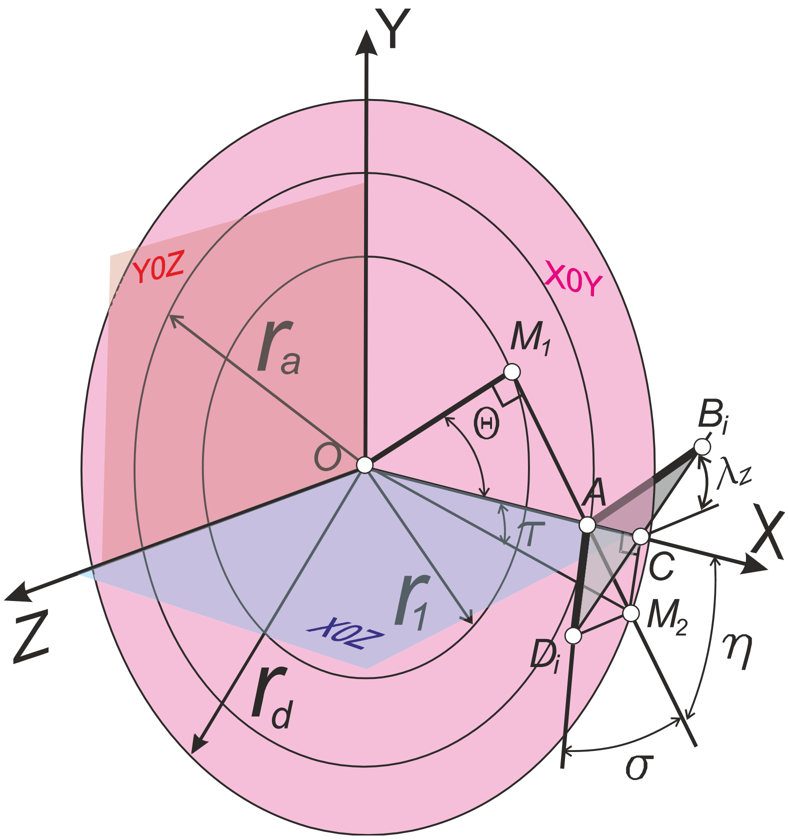

Figure 8. Scheme for calculating the deviation of the received profile of the convolute surface from the given profile of the thread.

The generator AD_i of the convolute screw crosses the X axis at point A, and it is inclined to the $X0Y$ plane at an angle σ. The projection of the generatrix AD_i on the $X0Y$ coordinate plane is the straight line AM_2, which forms an angle η with the X axis. The segment AD_i belongs to the creation and is the left cutting edge of the cutter. The right cutting edge AB_i together with the left AD_i form a flat rake surface of the B_iAD_i cutter, which is highlighted in gray. The B_iAD_i plane is inclined to the XZ plane at an angle λ.

In polar coordinates, which are part of the cylindrical system, the line AM can be defined by the rotation angle τ of an arbitrary point M_2, lying on this line around the origin of the coordinate system O, as well as the length of the radius vector OM_2.

In the $X0Z$ plane, similarly to formula (17), we obtain the analytical expression of the axial section of the convoluted helical surface:

$$Z(x) = tan(\sigma)x\frac{\sin\tau}{\sin\eta} - \frac{P}{2\pi}\tau, \tag{18}$$

where:

τ is one of the curvilinear coordinates of the cutting edge, determined by the formula

$$\tau = \eta - arcsin\left(\frac{r_a \sin\eta}{x}\right); \tag{19}$$

P is the pitch of the specified thread.

Since the input data are the angle of inclination of the cutting edge λz and the height of the fundamental triangle of the cut H, the functional dependence of the values η and σ on them should be detected.

According to Figure 1:

$$|DC| = \frac{P}{2}, \qquad |AC| = H - \frac{Ptan(\varphi)}{2} = \frac{2H - Ptan(\varphi)}{2}.$$

Preprints.org (www.preprints.org) | NOT PEER-REVIEWED | Posted: 12 March 2024 doi:10.20944/preprints202403.0719.v1

Since the cutter is full-profile, then

$$|D_iC| = |DC| = \frac{P}{2},$$

From the triangle CD_iM_2 (Figure 8) we have $|CM_2| = \frac{P\sin\lambda_z}{2}$.
From the triangle ACM_2 we have $tan(\eta) = \frac{|CM_2|}{|AC|}$. So:

$$\eta = arctan\left[\frac{\frac{P\sin\lambda_z}{2}}{\frac{2H-Ptan(\varphi)}{2}}\right] = arctan\left(\frac{P\sin\lambda_z}{2H-Ptan(\varphi)}\right). \quad (20)$$

From the triangle D_iAM_2 we get the following ratios

$$tan(\sigma) = \frac{|D_iM_2|}{|AM_2|}.$$

At the same time:

$$|D_iM_2| = |D_iC|\cos\lambda_z,$$

$$|AM_2| = \frac{|AC|}{\cos\eta} = \frac{2H-Psin(\varphi)}{2\cos\eta}.$$

So:

$$tan(\sigma) = \frac{P\cos\lambda_z\cos\eta}{2H-Ptan(\varphi)} = \frac{P\cos\lambda_z}{2H-Ptan(\varphi)}\cos\left(arctan\left(\frac{P\sin\lambda_z}{2H-Ptan(\varphi)}\right)\right). \quad (21)$$

Analytical dependences (18) – (21) obtained in this way describe the axial section of the convolute helical surface, which is obtained by a cutter with a non-zero angle of inclination of the cutting edge.

The obtained dependences (18) – (21) under the condition of zero value of the angle λ_z describe the profile of the Archimedean screw according to equation (1).

However, $\tau = 0$, $\frac{\sin\tau}{\sin\gamma} = 1$, and $\frac{P}{2\pi}\tau = 0$, $tan(\sigma) = \frac{P}{2H} = \alpha$, if λ_z approaches 0 and then equation (18) becomes equivalent to equation (1).

The study [58] proves the functional influence of the angle of inclination of the grinding tool on the profile of the resulting screw and proposes an algorithm for obtaining the axial profile of a polished worm screw. The angle of inclination of the grinding profile tool is one of the parameters of the methodology and application support presented in the study [59] for accurate processing of conical worm screws with various curved axial profiles.

Profiling of tools for the process of whirling turning of worm shafts *ZA* (Archimedean profile) and *ZI* (involute profile) is presented in the study [60]. This work does not contain analytical studies on convoluted helical surfaces. Functional dependencies of worm surface profiles and cutting-edge profiles of tools for their production, the rake angle always has only zero value.

Therefore, the combined influence of the angle of inclination of the cutting edge and the rake angle of the tool on the value and accuracy of the half-profile angle based on the convolute approach to the formation of the conical large-pitch thread is an unsolved problem. Therefore, the goal of this study is to build an analytical model of profiling a triangular conical section using cylindrical coordinates and its verification based on the created algorithm and thread profile computer modeling. Attention should be paid to the fact that the cylindrical coordinates most accurately correspond to the model of the formation of helical surfaces, since they fully correspond to the movements of forming: the translational movement of the cutting edges along the *Z* axis of the thread, and at the same time their rotational movement around it.

3. Mathematical Modelling of the Profile Flanks of the Tool-Joint Drill-String Tapered Thread, as a Function of the Geometric Parameters of the Cutting Tool with a Double Inclination of the Rake Plane: Rake Angle and Inclination of Cutting Edge

Since the drill-string thread is tapered, the fundamental triangle thread *BAD* (Figure 1) has its sides of not the same in length.

Preprints.org (www.preprints.org) | NOT PEER-REVIEWED | Posted: 12 March 2024 doi:10.20944/preprints202403.0719.v1

Length of long side *AB*:

$$|AB| = \frac{H \cdot \cos\varphi}{\sin(2\alpha - \varphi)}. \quad (22)$$

Length of short side *AD*:

$$|AD| = \frac{H \cdot \cos\varphi}{\sin(2\alpha + \varphi)}, \quad (23)$$

where φ is the taper angle of the thread.

These formulas are necessary to establish the desired algorithm in relation to the drill-string tapered thread.

Therefore, the calculation scheme for placing the plane of the rake surface of the AB_iD_i of the lathe cutting tool (light pink color) is built in the cylindrical coordinate system and the Cartesian coordinate system *XYZ* combined with it, with the coordinate planes *X0Z* (purple color), *Y0Z* (lime color), *X0Y* (pink) (Figure 9).

3.1. Placement of the Rake Plane of the Lathe Thread Cutting Tool in the Cylindrical and Cartesian Coordinate System

Mutually perpendicular segments (D_iS_i) and (AC_i) are placed on the front plane. The segments intersect at the point E_i. Points A, E_i, C_i lie in the coordinate plane *X0Y* (pink). The angle between the axis *X* and the straight line AC_i is the rake angle γ at point *A*. The segment Ad' is the projection of the segment AD_i on the *XOY* plane. The segment Ab' is the projection of the segment AB_i on the plane *XOY*. Each of the specified projections is inclined to the *X* axis at angles η and η_1, respectively. The length of the segment D_id' is the applicate (coordinate on the *Z* axis) of the point D_i. The length of the segment D_ib' is the applicate (coordinate on the *Z* axis) of the point B_i.

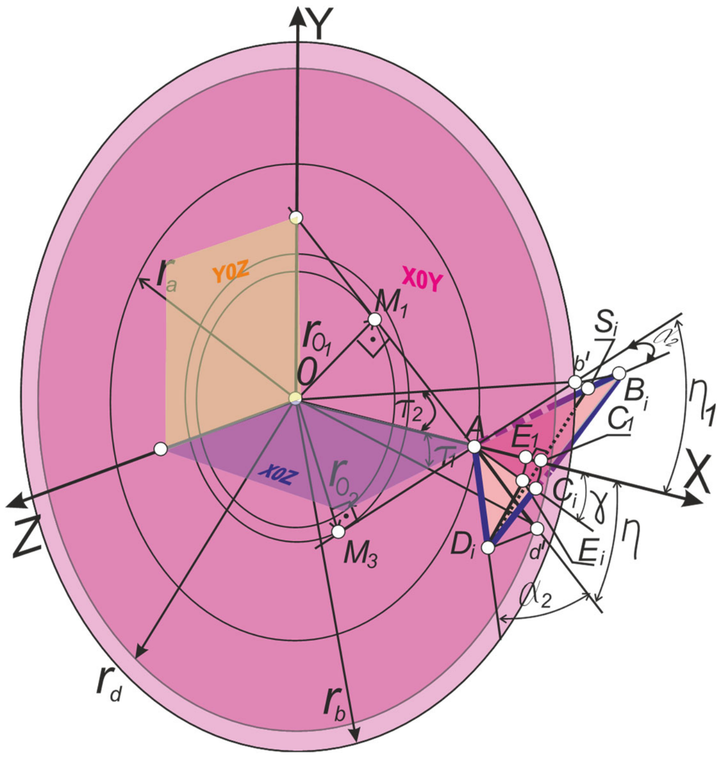

Figure 9. Scheme of placing of the rake plane of the AB_iD_i cutting tool in the cylindrical coordinate system.

The segment AD_i is the left-hand cutting edge of the cutter, and therefore the generator of the helicoid. It is placed at an angle α_2 to the *X0Y* plane. Segment AB_i is the right-hand cutting edge of the cutter, and therefore it is also the generating edge of the screw. It is also placed at an angle α_2 to the *X0Y* plane. For ordinary cutters, the values of these angles are equal to the standard half-profile angle $\alpha = 30°$. Point M_1 is the point of contact of line $d'M_1$ to the main cylinder with radius r_{o1}. Point M_2 is the point of contact of the line $b'M_2$ to the main cylinder with radius r_{o2}. The angle τ is the polar angle of an arbitrary point of the segment Ad', and the angle τ_1 is the polar angle of an arbitrary point of the segment Ab' (Figure 9, Figure 10).

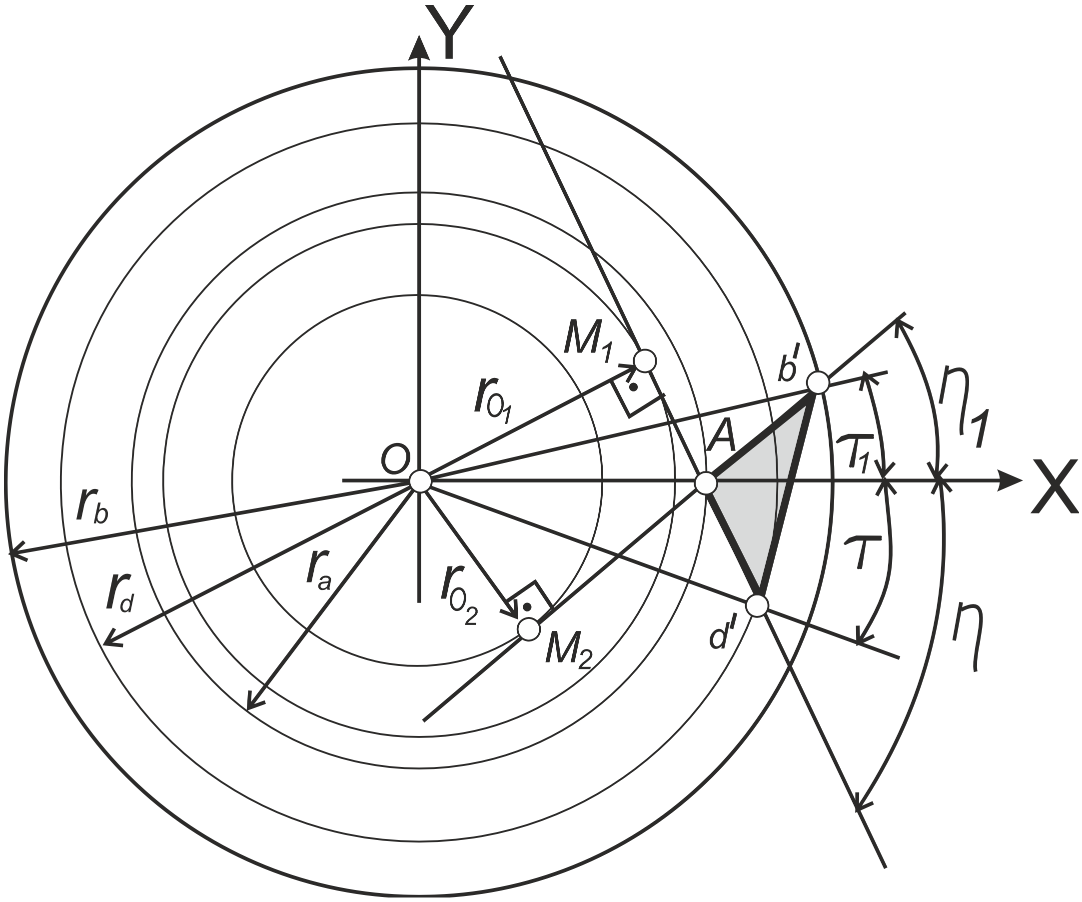

Figure 10. Diagram of placement of the rake plane projection of the lathe tool $A\ b'd'$ in the polar coordinate system.

3.2. Determination of The Axial Cross-Section of Tapered Thread as a Convoluted Helical Surface Depending on the Geometric Parameters of the Lathe Cutter: the Rake Angle at the Nose and the Inclination Angle of the Cutting Edge

So, by analogy with formula (14), the Z coordinates of the points of the generating AD_i depending on the angle of rotation τ, the X coordinates and the value of the radius r_a can be found by the equation:

$$Z(x) = tan(\alpha)x\frac{\sin\tau}{\sin\eta} - \frac{P}{2\pi}\tau, \tag{24}$$

where:

$$\tau = \eta - arcsin\left(\frac{r_a \sin\eta}{x}\right). \tag{25}$$

So, by analogy with formula (14), the Z coordinates of the points of the generating AB_i depending on the angle of rotation τ_1, the X coordinates and the value of the radius r_b can be found by the aquation:

$$Z(x) = tan(\alpha)x\frac{\sin\tau_1}{\sin\eta_1} - \frac{P}{2\pi}\tau_1, \tag{26}$$

where:

Preprints.org (www.preprints.org) | NOT PEER-REVIEWED | Posted: 12 March 2024 doi:10.20944/preprints202403.0719.v1

$$\tau_1 = \eta_1 - arcsin\left(\frac{r_a \sin\eta_1}{x}\right). \quad (27)$$

For the completeness of expressions (24-27), it is necessary to establish the algorithms for finding angles η, η_1.

3.2.1. Definition of Angles η and η1

3.2.1.1. A Sketch of the Front Plane of the Cutting-Tool as a Plane of General Position in Cartesian Coordinates

In Figure 11 shows a complex drawing of the plane *ABD* of the rake surface of the thread cutting tool of the general position. The projection plane π_1 corresponds to the reference plane at the nose point *A*. Through point *A*, the *X* axis is drawn, which corresponds to the *X* axis illustrated in Figure 9 and Figure 10. The axes *Y* and *Z* also correspond to the axes of the same name in Figure 9. The *XOY* plane is parallel to the frontal plane of the π_2 projections. The plane *XOZ* coincides with the main reference plane at point *A*, i.e. it is parallel to the horizontal plane of projections π_1. The *YOZ* plane is parallel to the π_3 projection plane.

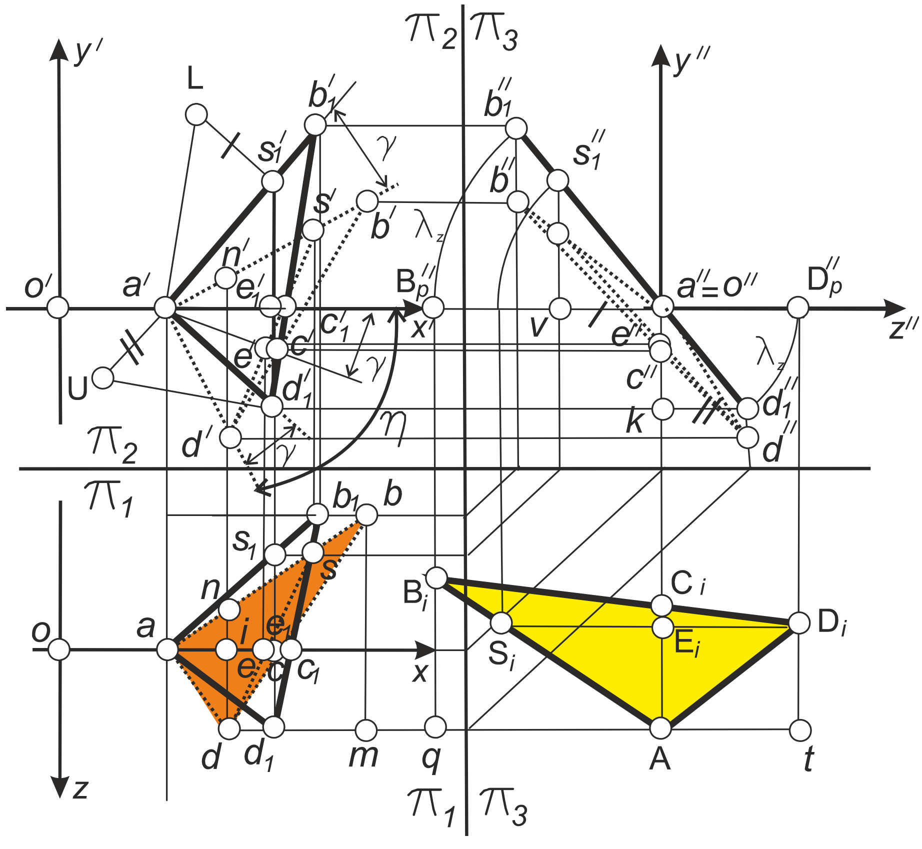

Figure 11. Complex drawing of the plane of the rake surface *ABD* of the lathe tool, which is placed under the angle of inclination λ_z and the rake angle at the nose point γ.

The rake plane of the cutting tool AB_1D_1 is constructed as a plane that is perpendicular to the plane of projections π_3. This plane is marked with bold lines. Its projection onto the π_3 plane is denoted by $b_1''a''d_1''$. The natural value of the angle λ_z is placed on the projection plane π_3. This angle corresponds to the angle of rotation of the specified plane around the *X* axis. Considering the fact that the *Z* axis in the cylindrical coordinate system is constructed as the axis of the screw thread, it means that the angle λ_z is the angle of setting the plane AB_1D_1 relative to the plane of the axial section of the screw.

Within the AB_1D_1 plane, the segment AC_1 is constructed, which lies on the *X* axis and the segment D_1S_1 is perpendicular to it. The segments intersect at point E_1.

Preprints.org (www.preprints.org) | NOT PEER-REVIEWED | Posted: 12 March 2024 doi:10.20944/preprints202403.0719.v1

The rotation of the plane AB_1D_1 by an angle γ is carried out in the plane *XOY*, which coincides with the reference plane at point *A*. Thus, all points of the plane AB_1D_1 are rotated by an angle γ around an axis that is parallel to the *Z* axis and passes through point *A*. Therefor on the π_2 projection plane, the angle γ is reflected in its natural form. As a result of the rotation, the plane *ABD* was formed (it is highlighted with dashed lines). The specified plane is the desired plane of the rake surface of the thread cutting tool, and its horizontal projection *abd* (orange) corresponds to the given fundamental triangle of the tapered thread *ABD* from Figure 1 and Figure 2.

The natural appearance of the triangle of the cutting edge of the cutter, which is intended to form the fundamental triangle *ABD*, is shown in Figure 11 in the form of a triangle AB_iD_i (yellow). The specified triangle is constructed by combining the projection $a''b_1''d_1''$ with the plane *XOZ*, i.e. by turning the plane AB_iD_i around the *X* axis by an angle λ_z, which is naturally equal to the lead angle of the helix ψ.

3.2.1.2. Trigonometric Definition of an Angle η and η_1.

The angle η is the angle of inclination of the frontal projection of the cutting edge AD_i to the *XOZ* plane (Figure 9), which means $a'd_1'$ to the x' axis (Figure 10, Figure 11). It can be defined as the sum of the angle γ and the angle $d_1'a'e_1'$. So, we will determine the indicated angle according to the equation:

$$\eta = \gamma + \angle d_1^{'}\alpha' e_1^{'}. \tag{28}$$

From the right triangle $d_1'a'e_1'$, the angle $d_1'a'e_1'$ can be determined using the following formula:

$$\angle d_1'a'e_1' = arctan\left[\frac{|d_1'e_1'|}{|a'e_1'|}\right], \tag{29}$$

where:

$|d_1'e_1'|$ equals $|a''k|$ (Figure 11), that can be determine from right triangle $d_1''ka''$ as follows:

$$|d_1'e_1'| = |a''k| = tg(\lambda_z)|kd_1''| = tg(\lambda_z)|di|, \tag{30}$$

where:

|di| is determined from right triangle *dai* (Figure 11):

$$|di| = sin(\angle dai) \cdot |ad| = sin(\alpha)|AD|. \tag{31}$$

So, after inserting equation (31) into it, formula (30) will look like this:

$$|d_1'e_1'| = tan(\lambda_z)sin(\alpha)|AD|. \tag{32}$$

$|a'e_1'|$ is defined from right triangle $d_1'a'e_1'$ due to expression (Figure 11):

$$|a_1'e_1'| = \sqrt{|a_1'd_1'|^2 - |d_1'e_1'|^2}, \tag{33}$$

where:

$|d_1'e_1'|$ is defined by equation (30);

$|a'd'_1|$ can be determined using a right triangle $ua'd'_1$, in which the segment (ua') is set at right angles to the segment $a'd'_1$ and its size is equal to the length of the segment kd''_1, i.e. equal to the difference in the coordinates of the points *k* and d''_1 in the plane of projections π_3.

Based on the method of finding the actual values of the segment lengths in the sketch geometry, the constructed right triangle contains the segment ud'_1, which is the real value of the segment AD_i, i.e. it is the real value of one of the two lateral cutting edges of the cutter. Since in Figure 11 the real appearance of the triangle of the cutting edge of the cutter is displayed as AB_iD_i figure, then we have the following expression:

$$|ud_1'| = |AD_i|.$$

Thus, the length of the segment $a'd'_1$ from the triangle $ua'd'_1$ will be determined by the following equation:

Preprints.org (www.preprints.org) | NOT PEER-REVIEWED | Posted: 12 March 2024 doi:10.20944/preprints202403.0719.v1

$$|a'd_1'| = \sqrt{|ud_1'|^2 - |ua'|}^2 = \sqrt{|AD_i|^2 - |kd_1''|^2}, \tag{34}$$

where:

$$|kd_1''| = |a''d_1''| \cdot cos\,\lambda_z,$$

where:

$$|a''d_1''| = |E_iD_i| = |AD_i| \cdot sin(\angle E_iAD_i).$$

So, taking into account that the profile of the cutting edge and thread profile are the same, i.e. $|AD_i|=|AD|$, we get follow expression:

$$|a'd_1'| = |AD|\sqrt{1 - sin^2\,\alpha\,cos^2\,\lambda_z}. \tag{35}$$

Thus, formula (33) will take the following form:

$$|a_1'e_1'| = \sqrt{(|AD|\sqrt{1 - sin^2\,\alpha\,cos^2\,\lambda_z)}^2 - (tan(\lambda_z)sin(\alpha)|AD|)\,^2}.$$

And after certain manipulations, this equation received the following definition:

$$|a_1'e_1'| = \;|AD|\,\sqrt{1 - sin^2\,\alpha(\,cos^2\,\lambda_z - tan(\lambda_z)^2)}. \tag{36}$$

According to formulas (28), (29) and taking into account expressions (32), (33), (37) η defines as follows:

$$\eta = \gamma + arctan\left(\frac{tan(\lambda_z)sin(\alpha)}{\sqrt{1 - sin^2\,\alpha(\,cos^2\,\lambda_z - tan(\lambda_z)^2)}}\right). \tag{37}$$

Using Figure 11 in similar way, the formula for determining the angle η_1 can be derived:

$$\eta_1 = arcsin\left(\frac{sin\,\alpha\,sin\,\lambda_z}{\sqrt{1 - sin^2\,\alpha\,cos^2\,\lambda_z}}\right) - \gamma. \tag{38}$$

So, the group of equations (24-27) and (38) is the mathematical model of the side profile of a tapered thread with a given triangular or trapezoidal profile, which is a function of the thread diameter and pitch, as well as the geometric parameters of the cutting tool: the rake angle, the angle of inclination and the half-profile angle of its cutting edge.

According to formula (38), the angle $\eta=\eta_1=0$, if $\gamma=\lambda_z=0$, and therefore according to formulas (24, 25): $Z(x)=tan(\alpha)x$, which corresponds to formula (1).

4. Modelling of a Tapered Thread Profile for Drill-Strings

On the basis of the algorithm (24-27, 38), a visual application program was developed for obtaining the calculated drill-string tool-joint thread profile, the standard sizes of which are regulated by the standard [59]. The standard regulates 31 standard sizes of tool-joint tapered threads, which are formed as external threads for the pin (Figure 12 (a)) and as internal threads for the box (Figure 12 (b)).

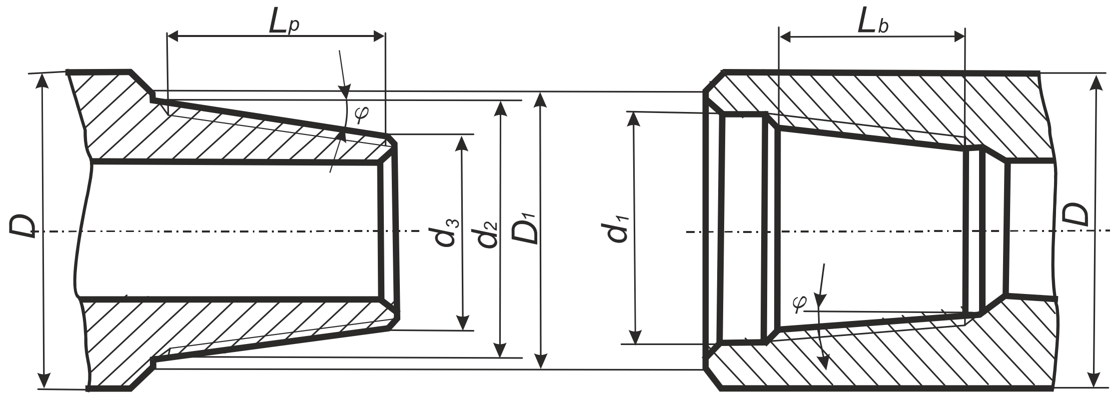

(**a**) (**b**)

Figure 12. Drawing of the drill-string tool-joint parts of the pin (**a**) and the box (**b**): φ is the taper angle, D is the outer diameter of the tool-joint tapered thread, D_1 is the diameter of the tool-joint tapered thread on the end section, d_1 is the diameter of the cylindrical twist, d_2 is the diameter of the larger base of the cone, d_3 is the diameter of the smaller base of the cone, L_p is the length of the threaded part of the pin, L_b is the length of the threaded parts of the box.

4.1. Geometrical Model of NC23 Drill-String Tool-Joint Thread Profile

The example concerns the standard size of the tool-joint thread NC23 based on the application of a special visual application program developed by the authors of this paper (Onysko, Kopey) based on the application of the algorithm (24 – 27, 38). The program provides for calculating the coordinates of the points of rectilinear sections - the sides of the thread fundamental triangle *AB* and *CD* (Figure 1). The input data for calculating the coordinates of the points of the thread fundamental triangle are the values of the parameters of a certain standard size and the values of the rake angle γ and the inclination angle of the cutting edge λ. This modelling example concerns one of the most common threaded profiles in the practice of using drill strings V-0.038R (Table 1). This profile is used for the NC23 drill-string thread, which has the smallest diameter of the smaller base of the cone d_3 and at the same time the largest value of the step P, which means the largest value of the thread lead angle ψ, which is usually close or equal to the inclination angle of the cutting edge λ.

Table 1. Profile parameters of the drill-string tool-joint tapered thread NC23 according to the standard [43].

No	Parameter name, dimension	Marking	Value
1	Pitch, mm	P	6.35
2	Tapered angle, °	φ	4.763
3	Thread height (not truncated), mm	H	5.487
4	Thread height (truncated), mm	h	3.095
5	Root truncation, mm	f_c	1.427
6	Crest truncation, mm	f_r	0.965
7	Angular depth, mm	h_1	2.633
8	The outer thread diameter of the small base of the cone of pin, mm	d_3	52.433
9	Half-profile angle, °	α	30

It is convenient to place the original point (0, 0) of the orthogonal coordinate system *XZ* for determining the profile of the thread on the axis of the thread and in relation to the root of the first turn at the point corresponding to the coordinate of point *A* on the *Z* axis (Figure 13). Therefore, Z_a=0. For the convenience of profiling and evaluation of the profiled longer and shorter flanks of the thread, two opposite oriented axes are used: - Z and +Z (Figure 13). The points of thread fundamental triangle

Preprints.org (www.preprints.org) | NOT PEER-REVIEWED | Posted: 12 March 2024 doi:10.20944/preprints202403.0719.v1

are signed as in Figure 1: *A*, *B*, *D* and an additional point *C*. The points of the thread profile that indicate its straight sections are marked by numbers: (3, 4) are points of the smaller flank, (5, 6) are points of the larger flank. The half-profile angles of the tool cutting- edge are the same and have the designation α_1. For ordinary cutting-tools it is obvious that α_1 is equal 30°. Half-profile angles of the obtained thread are signed differently: α_l is the half-profile angle formed by the larger flank of the thread profile, α_{sh} is the half-profile angle formed by the smaller flank of the thread profile.

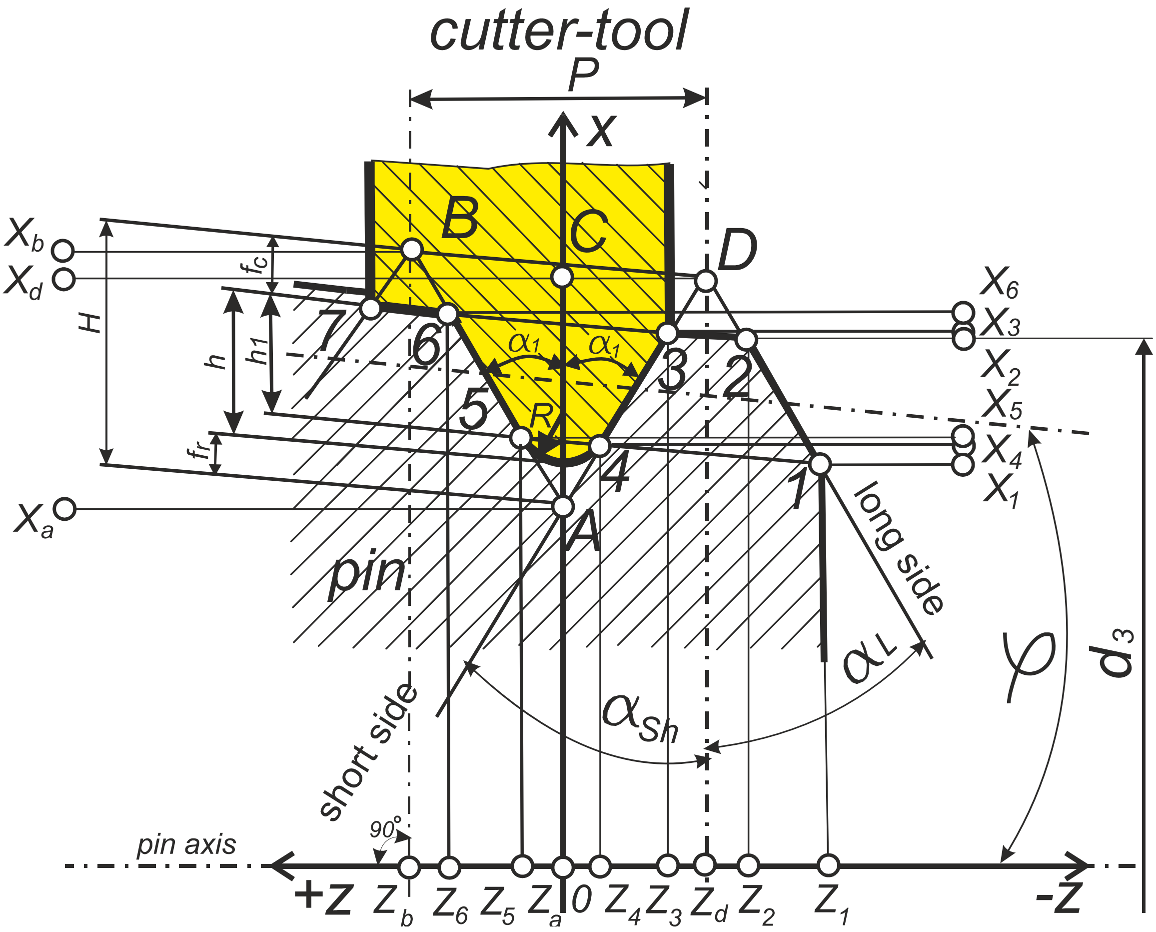

Figure 13. Scheme of obtaining the profile of a drill-string thread, which is made using the full-profile lathe thread cutting-tool (yellow).

With such a coordinate plan, the coordinates of the vertices of the fundamental triangle for each thread turn *n* can be determined by the following formulas:

$$X_a = nP\tan(\varphi) + d_3/2 + f_c - H, \text{ (mm)}, \quad (39)$$

$$X_d = nP\tan(\varphi) + d_3/2 + f_c + \tan(\varphi)F_r/2, \text{ (mm)}, \quad (40)$$

$$X_b = X_a + H + \tan(\varphi)P/2, \text{ (mm)}. \quad (41)$$

4.2. Modeling of the Fundamental Triangle Profile of the NC23 Drill-String Tapered Thread Obtained Using Turning-Tool at Its Zero Parameters: Rake Angle γ and the Inclination Angle of the Cutting Edge λ

According to aquations (39-41), the *X* coordinates of the vertices of the fundamental triangle *A*, *B*, *D* are as follows (Figures 14 and 15):

X_a=22.16 mm, X_d =27.65 mm, X_b = 27.93 mm.

Basing on the algorithm (24 – 27, 38) and the data X_a, X_d, X_b as well as the values γ=0 and λ_z=0, the values of the Z coordinates of the vertices of the fundamental triangle A, B, D were obtained: Z_d = 3.17 mm (Figure 14), Z_b=3.33 mm (Figure 15).

Diagrams (Figures 14 and 15) obtained on the basis of visualization of the algorithm (24 – 27, 38) show the rectilinear nature of the lateral fundamental profile of the NC23 thread under the condition of using a conventional threaded cutter with zero values of the rake angle γ=0 ° and the angle of inclination of the cutting edge λ=0°.

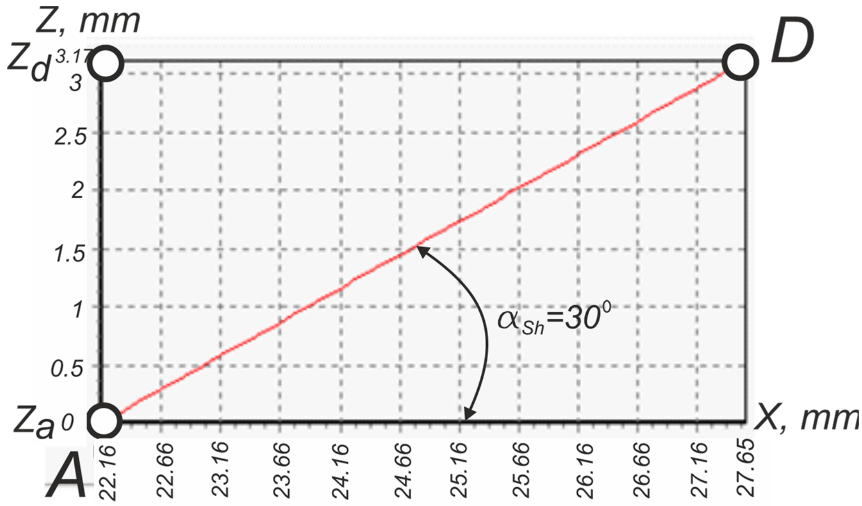

Figure 14. Visual software model of the flank profile *AD* of the drill-string tool-joint thread NC23.

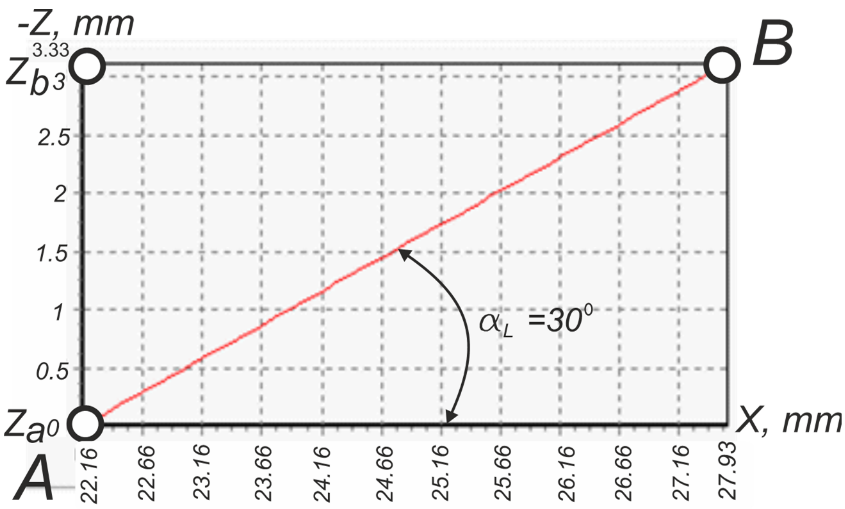

Figure 15. Visual software model of the flank profile *AB* of the drill-string tool-joint thread NC23.

The exact values of the coordinates Z_d = 3.17 mm and Z_b = 3.33 mm were obtained using algorithm (24 – 27, 38). Half-profile angles α_L, α_{sh} (Figures 14 and 15) are determined by the formulas:

$$\alpha_L = arctan\left(\frac{z_b}{x_b - x_a}\right), \tag{42}$$

$$\alpha_{sh} = arctan\left(\frac{z_d}{x_d - x_a}\right). \tag{43}$$

After substituting the data: X_a = 22.16 mm, X_d = 27.65 mm, X_b = 27.93 mm, Z_d = 3.17 mm, Z_b = 3.33 mm in formulas (42, 43) we get:

$$\alpha_L = \alpha_{Sh} = \alpha = 30° \text{ (Figure 14, Figure15, Figure 1).}$$

Preprints.org (www.preprints.org) | NOT PEER-REVIEWED | Posted: 12 March 2024 doi:10.20944/preprints202403.0719.v1

That is, both angles have the value prescribed by the standard. Therefore, according to equation (1), the graphs in Figures 14 and 15 show the algebraic linear dependence:

$$Z(x) = tan\left({}^{\pi}/_{6}\right)x = 0.58x. \quad (44)$$

4.3. Modeling of the NC23 Drill-String Tool-Joint Thread Profile Obtained Using Thread-Turning Tool with Its Geometric Parameters: Rake Angle γ=50° and Inclination Angle of the Cutting Edge λz=2.61°

4.3.1. Modelling of the Flank Part of Profile of the Thread

The inclination angle of the cutting edge λ_z is defined as equal to the lead angle of the screw on the outer diameter at a given turn of the thread ψ_3 (Figure 7), which is determined by the formula:

$$\psi_3 = arctan\frac{P}{\sqrt{(P\cdot tan(\varphi))^2+\pi^2\left(d_3+2l\cdot tan(\varphi)\right)^2}}, \quad (45)$$

where l is the distance from the smaller base of the cone to a specific turn of the thread.

The value of the thread lead angle ψ_3 can be determined at any distance l from the smaller base of the cone of the tapered thread to its larger base. If the distance l=0, then the lead angle of is maximum and its effect on the nature of the profile curve is obviously maximum (45). For the NC23 thread, it is ψ_3 = 2.61°. Therefore, it is accepted that inclination angle of cutting edge is equal to this one: $\lambda_z = \psi_3$ = 2.61°.

For reasons of graphical persuasiveness of the influence of the rake angle on the character of the side profile of the obtained thread, an excessively large value of the rake angle γ=50° was adopted (Figure 16).

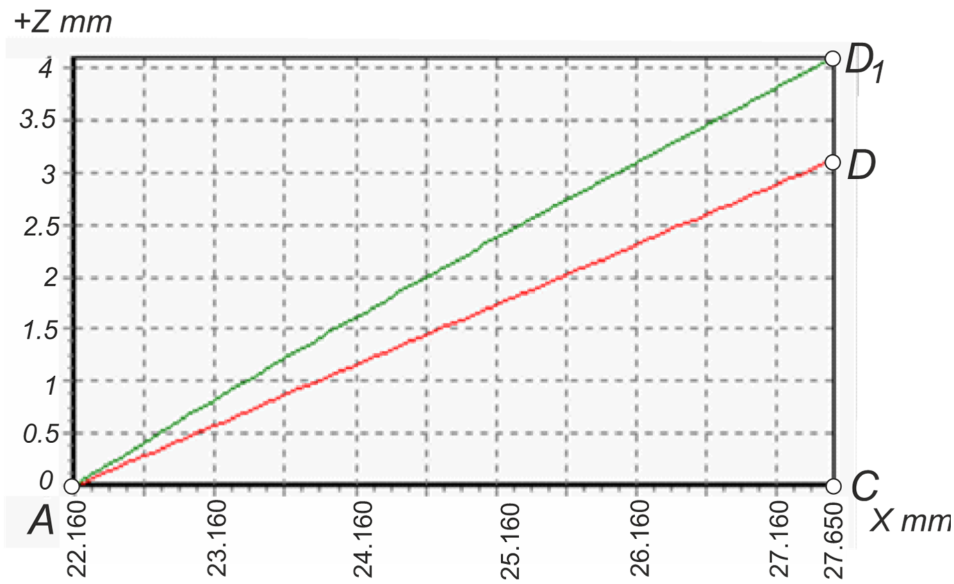

Figure 16. Comparison of models of the lateral theoretical profile of the NC23 thread: standard (red) and made by the tool with the geometric parameters of the cutter γ=50°, λ_z=2.61° (green).

4.3.2. Analysis of the Flank Profile Models of Thread

The large visual difference between the standard profile and the predicted profile obtained under the condition of using the parameters γ=50°, λ_z=2.61 proves the importance of analyzing the obtained data. The red line *AD* is the standard view of the side profile of the starting triangle of the conical keyhole. The inclination angle of the line *AD* relative to the *X* axis is 30°, which corresponds to the standard value of the thread half-profile angle α_{sh} near its short side (Figure 17).

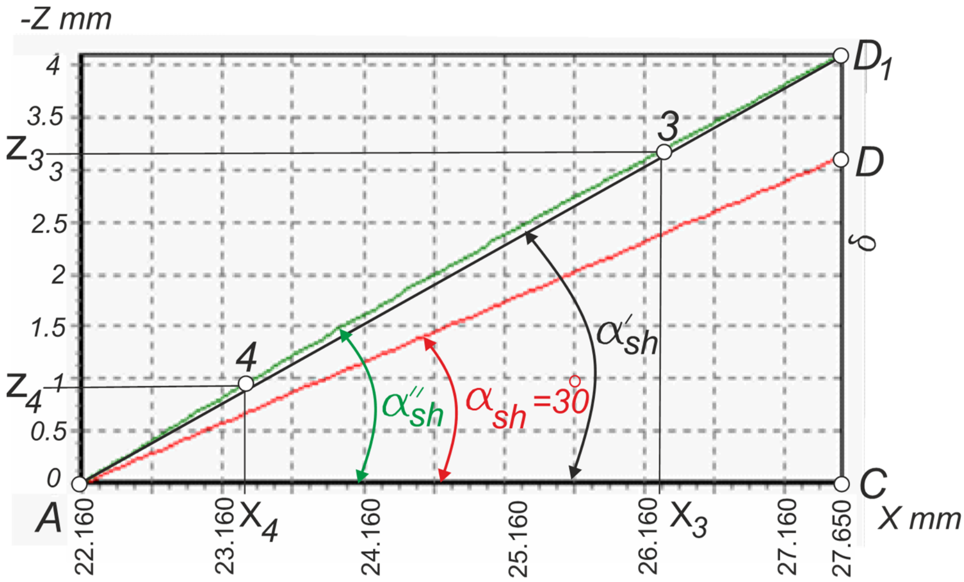

Figure 17. Comparison of models of the side profile of the NC23 thread: red straight *AD* – standard, green curve AD_1 – predicted profile obtained using the tool with geometric parameters of the cutter γ=50°, λ_z=2.61°, black straight AD_1 linear interpolation of the green curve by two points.

The green line AD_1 is a curve obtained according to the algorithm (24 – 27, 38) of the profile of the fundamental triangle side according to the applied parameters of Table 1 and the geometric parameters of the cutting tool γ=50°, λ_z=6.51°. The black line AD_1 is an interpolation of the two extreme points of the green curve. It is inclined to the *X* axis at an angle α_{sh}, according to formula (43), and therefore the straight line AD_1 is described by the equation (Figure 15):

$$Z = \tan(\alpha_{sh}{'}) = \frac{|CD_1|}{|CA|} = \frac{(z_{d1-} z_C)}{(X_C - x_A)} x. \tag{45}$$

By analogy, the line AB_1 is described by the equation:

$$Z = \tan(\alpha_{l}{'}) = \frac{(z_{B1-} z_C)}{(X_C - x_A)} x. \tag{46}$$

It is more correct to define the profile angle as the angle of inclination not of the lateral side *AD*, which refers to the original theoretical (fundamental) triangle, but of the lateral side between points *3* and *4* (Figure 13), which is actually part of the thread profile. On the diagram, Figure 17 is line (*34*), which is part of the green AD_1 curve. If we take it as a segment of the straight line (*34*) obtained by interpolation along the two extreme points *3* and *4*, then the section of the profile of the thread (*34*) can be described by the equation:

$$Z = \tan(\alpha_{sh}{''}) = \frac{(z_{3-} z_4)}{(X_3 - x_4)} x, \tag{47}$$

where the angle $\alpha_{sh}{''}$ is the actual thread half-profile angle along its shorter side, obtained by a cutter with non-zero geometric parameters.

With such orthogonal coordinate system, the coordinates of the vertices of the fundamental triangle for each turn of the thread *n* can be determined by the following formulas:

$$X_4 = X_d - f_c - h_1, \text{ (mm)}, \tag{48}$$

$$X_3 = X_d - f_c, \text{ (mm)}, \tag{49}$$

where X_d is obtained from formula (40).

Similarly, expressions can be obtained for determining the section of the actual thread between points 6 and 5 (Figure 13):

Preprints.org (www.preprints.org) | NOT PEER-REVIEWED | Posted: 12 March 2024 doi:10.20944/preprints202403.0719.v1

$$Z = \tan(\alpha_{l''}) = \frac{(z_6 - z_5)}{(X_6 - x_5)} x, \quad (50)$$

where the angle α_l'' is the predicted actual half-profile angle of the thread along its profile longer side, obtained by a cutter with non-zero geometric parameters.

$$X_5 = X_b - f_c - h_1, \text{ (mm)}, \quad (51)$$

$$X_6 = X_b - f_c, \text{ (mm)}, \quad (52)$$

where X_b is obtained from formula (41).

As a result of calculating the X coordinates according to formulas (48, 49) and (51, 52), as well as the corresponding Z coordinates based on the algorithm (24 – 27, 38), it is possible to give a predictive calculation of the half-profile angles of the NC23 thread obtained as a result its production with a cutting tool with geometric parameters: rake angle γ=50° and angle of inclination of the cutting edge λ_z=2.61°.

Table 2. Results of the predictive software calculation of half-profile angles of drill-string connecting thread NC23 α_{sh}', α_{sh}'', α_l', α_l'' obtained as a result of turning using a cutting tool with geometric parameters: rake angle γ=50° and inclination angle of the cutting edge λ_z=2.61 °.

Long side	Root	Short side	Short side truncate		Long side truncated	
mm						
X_{b1}	X_a	X_{d1}	X_3	X_4	X_5	X_6
27.93	22.16	27.65	26.22	23.59	23.87	26.50
Z_{b1}	$Z_a= Z_c$	Z_{d1}	Z_3	Z_4	Z_5	Z_6
4.73	0	4.17	3.42	1.28	1.52	3.64
Half- profile angles, °						
α_l'		α_{sh}'	α_{sh}''		α_l''	
39.34		37.22	39.14		38.87	

4.3.3. Modeling of the Side Profile of the NC23 Drill-String Connection Thread Made Using Turning Tool with Geometric Parameters: Rake Angle γ=12° and the Inclination Angle of the Cutting Edge λ_z=2.61°

In a case of turning stainless steel threads, researchers often recommend a rake angle in the range of 8-10° [45, 47]. The diagrams in Figures 18 and 19 show a certain visual difference between the actually straight standard profile and the side profile of the thread: *AB* in Figure 18 and *AD* in Figure 19. More precise numerical information obtained thanks to the predictive algorithm based on (24 – 27, 38) shows the possibility of using these geometric parameters: the rake angle γ=12° and the inclination angle of the cutting edge λ_z=2.61° for turning threads from difficult-to-machine materials and at the same time ensure the accuracy of the half-profile angle α=30±0.75° (Table 3). The values of the predicted half-profile angles α_{sh}'' = 30.04° and α_l''= 30.15° fall into this range and actually show that the excess of the angular size is less than 33% of the limit deviation tolerance. At the same time, it should be noted that the value of the angle α_l'= 30.58° indicates a deviation from the nominal, which reaches 73% of the tolerance. However, as can be seen from the diagram in Figure 17, the angles α_l', α_{sh}' have exclusively research value and actually prove the non-linear nature of the predicted flank profile of the NC23 thread obtained using thread turning with geometric parameters: rake angle γ=12° and angle of inclination of the cutting edge λ_z=2.61 °.

Preprints.org (www.preprints.org) | NOT PEER-REVIEWED | Posted: 12 March 2024 doi:10.20944/preprints202403.0719.v1

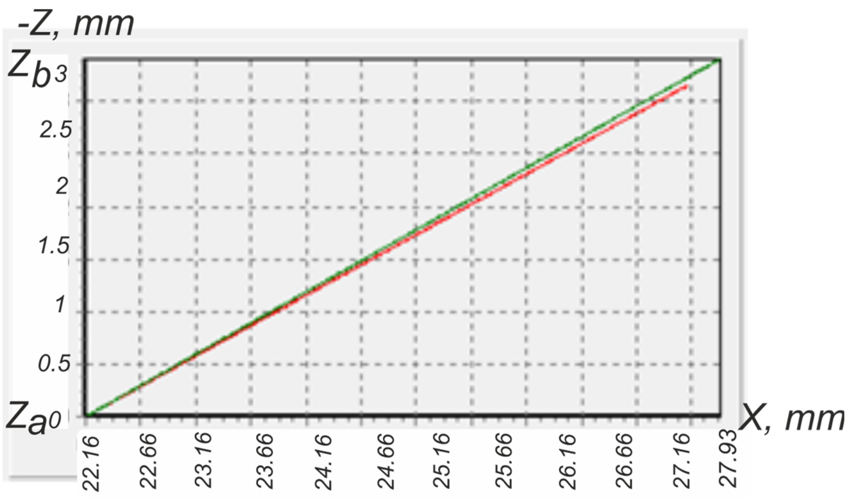

Figure 18. Comparison of the models of the side profile *AB* of the NC23 thread: standard (red) and made using the cutting tool with the geometric parameters of γ=12°, λ_z=2.61° (green).

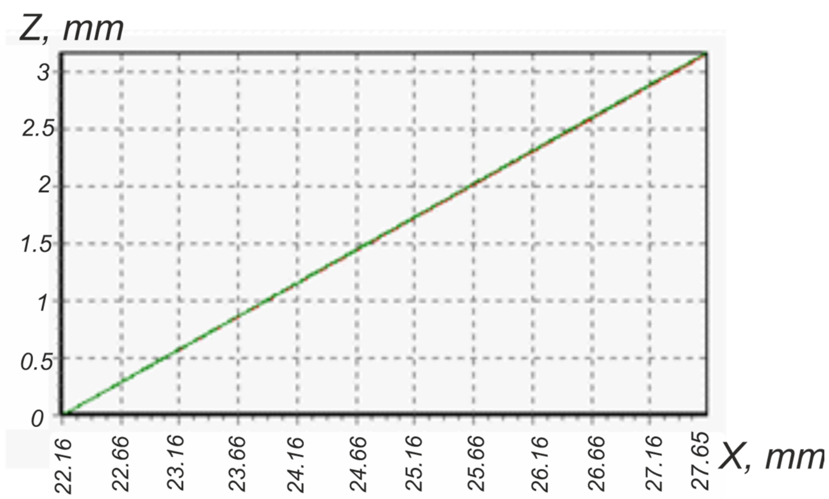

Figure 19. Comparison of the models of the side profile *AD* of the NC23 thread: standard (red) and made using the cutting tool with the geometric parameters of γ=12°, λ_z=2.61° (green).

Table 3. Results of the predictive software calculation of half-profile angles of NC23 drill-string thread α_{sh}', α_{sh}'', α_l', α_l'' made using tool with the rake angle γ=12° and the inclination angle of the cutting edge λ_z=2.61°.

Half- profile angles, °			
Side *AB*	**Side *AD***	**Flank 34**	**Flank 56**
α_l'	α_{sh}'	α_{sh}''	α_l''
30.58	30.08	30.04	30.15

4.4. The Results of Modelling the Side Profile of the NC56 Drill-String Thread Obtained Turning Cutting Tool with Geometric Parameters: Rake Angle γ = 8°, γ = -8°, γ = 4° and the Inclination Angle of the Cutting Edge λ_z = 1.06°

For a complete illustration of the effect of the diameter of the part on thread profile, let's use a drill-string thread of NC56 as example, the diameter of which is more than 117 mm (Table 4).

Preprints.org (www.preprints.org) | NOT PEER-REVIEWED | Posted: 12 March 2024 doi:10.20944/preprints202403.0719.v1

Table 4. Profile parameters of the drill-string tool-joint tapered thread NC56 according to the standard [41].

No	Parameter name, dimension	Marking	Value
1	Pitch, mm	P	5.471
2	Tapered angle, °	φ	7°,7′30′′
3	Thread height (not truncated), mm	H	5.471
4	Thread height (truncated), mm	h	3.083
5	Root truncation, mm	f_c	1.423
6	Crest truncation, mm	f_r	0.965
7	Angular depth, mm	h_1	2.625
8	The outer thread diameter of the small base of the cone of pin, mm	d_3	117.5
9	Half-profile angle, °	α	30

The results of the predictive calculation of the half-profile angles α_{sh}', α_{sh}'', α_l', α_l'' based on (24-27, 38) are presented in the Table 5. It refers to the application of values of rake angles γ = 8°, γ = -8°, γ = 4°, which are often recommended in scientific sources. The results show that the half-profile angle along the short side, is close in value for a negative and the same modulus of a positive rake angle. Half-profile angle, along the long sides, differ significantly when using positive or negative rake angles. However, the deviation from the nominal value by 0.35° does not exceed 47% of the ±0.75° angle tolerance. At the rake angle γ = 4°, the nominal deviation is less than 0.1°, which is 13% of the tolerance (Table 5).

Table 5. Results of the predictive software calculation of half-profile angles of NC56 drill-string thread α_{sh}', α_{sh}'', α_l', α_l'' obtained as a result of turning using cutting tool with geometric parameters: rake angle γ = 8°, γ = -8°, γ = 4° and the inclination angle of the cutting edge λ_z = 1.06°.

Parameters		Half-profile angles, °			
		Side *AB*	Side *AD*	Flank 34	Flank 56
λ,°	γ,°	α_l'	α_{sh}'	α_{sh}''	α_l''
1.060	-8	29.99	30.39	30.35	29.91
1.060	8	30.17	30.28	30.35	30.11
1.060	4	30.10	29.97	29.95	30.01

5. Conclusions

The triangular or trapezoidal shape of the profile specified by the standard cannot be performed for the surface of cylindrical and conical screw threaded parts, which are made with the help of turning cutters of high productivity. This is due to the kinematic and geometric features of the formation of helical surfaces, which are the flank surfaces of triangular, trapezoidal or rectangular threads. The guide lines of these surfaces are cylindrical or conical helixes, the creating of which is provided by the kinematics of the movement of the tool cutting edge points relatively to the workpiece. The straight-line part of the cutting edge of the lathe thread cutter is the generator of the helical surface. For the production of threaded parts from materials with different machinability characteristics, including difficult-to-machine alloy steels, there is a need to use specially oriented cutting edges relative to the axis of the parts. The such items have followed from this as a consequence:

• For an effective threading process on workpieces made of different machinability materials, cutters should be used with selected non-zero geometric parameters, namely the rake angle and the inclination angle of the cutting edge. It causes the surfaces of the conical or cylindrical threads performed with help of the specified cutters which consist of two convolute helicoids and the helical surfaces of the thread root and the thread crest connected to them;

 doi:10.20944/preprints202403.0719.v1

• The axial profile of the thread formed in this way does not contains rectilinear lateral flank, but only curved ones;

• The curvilinear profile of the lateral flanks is mathematically represented as a transcendental function, in which the parameters are the actual parameters of the thread: diameter, pitch as well as geometric parameters of the thread cutter: rake angle, half-profile angle and the inclination angle of its cutting edge;

• In case of using the known or scientifically justified values of the inclination angles of the edge and rake angles of turning cutters for threading, the obtained flank profile of the thread becomes close to rectilinear, and the value of the thread half-profile angles can be within the tolerance field for angular deviation;

• As the value of the tool rake angle and the inclination angle of the its cutting-edge decreases, as well as the threaded part diameter increases, the value of the predicted thread half-profile angle approaches the nominal value;

• In the case of using zero values of the geometric parameters of the thread turning cutter, the convolute helicoid as part of the thread surface changes to an oblique closed helicoid (Archimedes' screw), and its profile contains not curved, but straight flank lines;

• In the case of exactly zero values of the geometric parameters of the thread turning cutter: the inclination angle of the edge and the rake angle, the transcendental expression describing the lateral thread profiles turns into a linear algebraic equation describing the triangular, rectangular or trapezoidal profile of standard threads.

In nearest future it is planning to study the influence of setting deviation of lathe tool on thread profile accuracy.

Author Contributions: Conceptualization, O.O.; methodology, O.O., V.K. and V.P.; software, O.O. and V.K.; validation, J.K., M.B. and V.P.; formal analysis, V.K., S.B. and V.P.; investigation, O.O., C.B. and J.K.; resources, C.B., S.B. and P.D.; data curation, C.B., M.B. and P.D.; writing—original draft preparation, O.O.; writing—review and editing, P.D. and S.B.; visualization, M.B. and V.P.; supervision, V.P.; project administration, P.D. and V.P.; funding acquisition, C.B., S.B. and M.B. All authors have read and agreed to the published version of the manuscript.

Funding: This research was funded by Ministry of Education and Science of Ukraine, grant number PK 0124U000654.

Data Availability Statement: Not applicable.

Acknowledgments: The team of authors express their gratitude to the reviewers for their valuable recommendations that have been taken into account to significantly improve the quality of this paper.

Conflicts of Interest: The authors declare no conflicts of interest. The funders had no role in the design of the study; in the collection, analyses, or interpretation of data; in the writing of the manuscript; or in the decision to publish the results.

References

1. Wang, H.; Huang, H.; Bi, W.; Ji, G.; Zhou, Bo; Zhuo, L. Deep and ultra-deep oil and gas well drilling technologies: Progress and prospect. *Natural Gas Industry B* **2022**, *9(2)*, 141–157.
2. Sharmin, T.; Rodoshi Khan, N.; Md Saleh Akram; Ehsan, M. A. State-of-the-Art Review on Geothermal Energy Extraction, Utilization, and Improvement Strategies: Conventional, Hybridized, and Enhanced Geothermal Systems. *International Journal of Thermofluids* **2023**, *18*, 100323.
3. Wu, B.; Zhang, K.; Meng, G.; Suo, X. Optimization of Recharge Schemes for Deep Excavation in the Confined Water-Rich Stratum. *Sustainability* **2023**, *15*, 5432.
4. Klymenko, V.; Ovetskyi, S.; Vytyaz, O.; Uhrynovskyi, A.; Martynenko, V. An alternative method of methane production from deposits of subaquatic gas hydrates. *Mining of Mineral Deposits* **2022**, *16*, 11–17.
5. Bazaluk, O.; Slabyi, O.; Vekeryk, V.; Velychkovych, A.; Ropyak, L.; Lozynskyi, V. A technology of hydrocarbon fluid production intensification by productive stratum drainage zone reaming. *Energies* **2021**, *14*, 3514.
6. Chudyk, I.; Velychkovych, A.; Grydzhuk, Ja. A Modeling of the Inertia Properties of a Drill String Section as a Continual Bent Rotating Rod. *SOCAR Proceedings* **2021**, *2021 (4)*, 24–32.

7. Vlasiy, O.; Mazurenko, V.; Ropyak, L.; Rogal, O. Improving the aluminum drill pipes stability by optimizing the shape of protector thickening. *Eastern-European Journal of Enterprise Technologies* **2017**, *1(7–85)*, 25–31.
8. Chudyk, I. I.; Femiak, Ya. M.; Orynchak, M. I.; Sudakov, A. K.; Riznychuk, A. I. New Methods for Preventing Crumbling and Collapse of the Borehole Walls. *Naukovyi Visnyk Natsionalnoho Hirnychoho Universytetu* **2021**, *2021(4)*, 17–22.
9. Prysyazhnyuk, P.; Molenda, M.; Romanyshyn, T.; Ropyak, L.; Romanyshyn, L.; Vytvytskyi, V. Development of a hardbanding material for drill pipes based on high-manganese steel reinforced with complex carbides. *Acta Montanistica Slovaca* **2022**, *27*, 685–696.
10. Bembenek, M; Prysyazhnyuk, P.; Shihab, T.; Machnik, R.; Ivanov, O.; Ropyak, L. Microstructure and Wear Characterization of the Fe-Mo-B-C—Based Hardfacing Alloys Deposited by Flux-Cored Arc Welding. *Materials* **2022**, *15*, 5074.
11. Grydzhuk, Ja.S.; Dzhus, A.P.; Grydzhuk, Ja.S.; Dzhus, A.P.; Yurych, A.R.; Yurych, L.R.; Riznychuk, A.I.; Pylypaka, O.P. Approbation of the method for ensuring operational reliability and evaluating the residual life of drill string elements. In Proceedings of the 16th International Conference Monitoring of Geological Processes and Ecological Condition of the Environment, Monitoring 2022, 15-18 November 2022, Kyiv, Ukraine. European Association of Geoscientists & Engineers, EAGE 2022, 2022, pp. 1–5.
12. Onysko, O.; Kopei, V.; Kusyj, Y.; Kornuta, O.; Schuliar, I. Turning of NC10 Threads for Drill Pipes: Theoretical Study of the Designed Profile. In *Lecture Notes in Mechanical Engineering*. Advances in Design, Simulation and Manufacturing VI. DSMIE 2023; Ivanov, V., Trojanowska, J., Pavlenko, I., Rauch, E., Piteľ, J. Eds. Springer: Cham, Switzerland, 2023; pp. 356–366.
13. Kopei, V.; Onysko, O.; Kusyi, Y.; Vriukalo, V.; Lukan, T. Investigation of the Influence of tapered Thread Pitch Deviation on the Drill-String Tool-Joint Fatigue Life. In *Lecture Notes in Networks and Systems*, New Technologies, Development and Application V. NT 2022; Karabegović, I., Kovačević, A., Mandžuka, S. Eds.; Springer: Cham, Switzerland, 2023; Volume 472, pp. 144–154.
14. Shatskyi, I.; Ropyak, L.; Velychkovych, A. Model of contact interaction in threaded joint equipped with spring-loaded collet. *Engineering Solid Mechanics* **2020**, *8(4)*, 301–312.
15. Croccolo, D.; De Agostinis, M.; Fini, S.; Mele, M.; Olmi, G.; Scapecchi, C.; Tariq, M.H.B. Failure of Threaded Connections: A Literature Review. *Machines* **2023**, *11*, 212.
16. Ropyak, L.Y.; Vytvytskyi, V.S.; Velychkovych, A.S.; Pryhorovska, T.O.; Shovkoplias, M.V. Study on grinding mode effect on external conical thread quality. *IOP Conf. Ser. Mater. Sci. Eng*. **2021**, *1018*, 012014.
17. Mandryk, O.; Vytyaz, O.; Poberezhny, L.; Mykhailiuk, Y. Increase of the technogenic and ecological safety of the natural gas transportation due to displacement of explosive mixtures with nitrogen. *Archives of Materials Science and Engineering* **2020**, *106*, 17–27.
18. Wang, Y.; Qian, C.; Kong, L.; Zhou, Q.; Gong, J. Design Optimization for the Thin-Walled Joint Thread of a Coring Tool Used for Deep Boreholes. *Appl. Sci.* **2020**, *10*, 2669.
19. Grydzhuk, J.; Chudyk, I.; Velychkovych, A.; Andrusyak, A. Analytical estimation of inertial properties of the curved rotating section in a drill string. *East. Eur. J. Enterp. Technol.* **2019**, *1*, 6–14.
20. Pryhorovska, T.O.; Ropyak, L. Machining Error Influnce on Stress State of Conical Thread Joint Details. In Proceedings of the 8th International Conference on Advanced Optoelectronics and Lasers (CAOL 2019), Sozopol, Bulgaria. 6–8 September 2019; pp. 493-497.
21. Tutko, T.; Dubei, O.; Ropyak, L.; Vytvytskyi, V. Determination of Radial Displacement Coefficient for Designing of Thread Joint of Thin-Walled Shells. In *Lecture Notes in Mechanical Engineering*, Advances in Design, Simulation and Manufacturing IV. DSMIE 2021; Ivanov, V., Trojanowska, J., Pavlenko, I., Zajac, J., Peraković, D., Eds.; Springer: Cham, Switzerland 2021; pp. 153–162.
22. Onysko, O., Panchuk, V., Kusyi, Y., Odosii, Z., Lukan, T. Impact of the Tool's Flank Clearance Angle on the Pitch Diameter Accuracy of the Tool-Joint Tapered Thread. In *Lecture Notes in Mechanical Engineering*, Advances in Design, Simulation and Manufacturing V. DSMIE 2022; Ivanov, V., Trojanowska, J., Pavlenko, I., Rauch, E., Peraković, D. Eds.; Springer: Cham, Switzerland 2022; pp. 312–321.
23. Dubei, O.Y.; Tutko, T.F.; Ropyak, L.Y.; Shovkoplias, M.V. Development of Analytical Model of Threaded Connection of Tubular Parts of Chrome-Plated Metal Structures. *Metallofiz. Noveishie Tekhnol.* **2022**, *44*, 251–272.
24. Rong, L.; Tie, Z.; Wu, X.J.; Wang, C.H. Crack closure effect on stress intensity factors of an axially and a circumferentially cracked cylindrical shell. *Int. J. Fract.* **2004**, *125*, 227–248.
25. Shats'kyi, I.P. Closure of a longitudinal crack in a shallow cylindrical shell in bending. *Mater. Sci.* **2005**, *41*, 186–191.
26. Shats'kyi, I.P.; Makoviichuk, M.V. Analysis of the limiting state of cylindrical shells with cracks with regard for the contact of crack lips. *Strength Mater.* **2009**, *41*, 560–565.
27. Dovbnya, K.; Shevtsova, N. Studies on the stress state of an orthotropic shell of arbitrary curvature with the through crack under bending loading. *Strength Mater.* **2014**, *46*, 345–349.

Preprints.org (www.preprints.org) | NOT PEER-REVIEWED | Posted: 12 March 2024 doi:10.20944/preprints202403.0719.v1

28. Shats'kyi, I.P.; Makoviichuk, M.V. Contact interaction of crack lips in shallow shells in bending with tension. *Mater. Sci.* **2005**, *41*, 486–494.
29. Shatskii, I.P.; Makoviichuk, N.V. Effect of closure of collinear cracks on the stress-strain state and the limiting equilibrium of bent shallow shells. *J. Appl. Mech. Tech. Phys.* **2011**, *52*, 464–470.
30. Kopei, V.; Onysko, O.; Odosii, Z.; Pituley, L.; Goroshko, A. Investigation of the influence of tapered thread profile accuracy on the mechanical stress, fatigue safety factor and contact pressure. In *Lecture Notes in Networks and Systems*, New Technologies, Development and Application IV. NT 2021; Karabegović I. Eds.; Springer: Cham, Switzerland, 2021; Volume 233, pp. 177–185.
31. Kopei, V.B.; Onysko, O.R.; Panchuk, A.G.; Dzhus, A.P.; Protsiuk, V.R. Improving the fatigue life of the tool-joint of drill pipes by optimizing the variable pitch of the box thread. *IOP Conf. Series: Materials Science and Engineering* **2021**, *1166*, 012017.
32. Kopei, V.; Onysko, O.; Panchuk, V.; Pituley, L.; Schuliar, I. Influence of Working Height of a Thread Profile on Quality Indicators of the Drill-String Tool-Joint. In *Lecture Notes in Mechanical Engineering*, Grabchenko's international conference on Advanced manufacturing Processes. «InterPartner» 2021; Tonkonogyi V. at al. Eds.; Springer: Cham, Switzerland, 2022; pp. 395–404.
33. Onysko, O.; Borushchak, L.; Kopei, V.; Lukan, T.; Medvid, I.; Vryukalo, V. Computer Studies of the Tightness of the Drill String Connector Depending on the Profile of Its Tapered Thread. In *Lecture Notes in Networks and Systems*, New Technologies, Development and Application III. NT 2020; Karabegović I. Eds.; Springer: Cham, Switzerland, 2020; Volume 128, pp. 720–729.
34. Bazaluk, O.; Velychkovych, A.; Ropyak, L.; Pashechko, M.; Pryhorovska, T.; Lozynskyi, V. Influence of heavy weight drill pipe material and drill bit manufacturing errors on stress state of steel blades. *Energies* **2021**, *14*, 4198.
35. Kopei, V.B.; Onysko, O.R.; Panchuk, V.G.; Odosii, Z.M.; Kusyi, Y.M. Increasing the fatigue strength of threaded joints of oil and gas equipment by plastic deformation of the thread under high load before make-up. *J. Phys.: Conf. Ser.* **2023**, *2540*, 012033.
36. Litvin, F.; Gonzalez-Perez, I.; Yukishima, K.; Fuentes, A.; Hayasaka, K. Design, simulation of meshing, and contact stresses for an improved worm gear drive. *Mech. Mach. Theory* **2007**, *42*, 940–959.
37. Kusyi, Y.; Stupnytskyy, V.; Onysko, O.; Dragašius, E. Optimization synthesis of technological parameters during manufacturing of the parts. *Eksploatacja i Niezawodnosc* **2022**, *24(4)*, 655–667.
38. Ivchenko, O.; Ivanov, V.; Trojanowska, J.; Zhyhylii, D.; Ciszak, O.; Zaloha, O.; Pavlenko, I.; Hladyshev, D. Method for an Effective Selection of Tools and Cutting Conditions during Precise Turning of Non-Alloy Quality Steel C45. *Materials* **2022**, *15 (2)*, 505.
39. Petrakov, Y.; Danylchenko, M. A Time-Frequency Approach to Ensuring Stability of Machining by Turning. *Eastern-European Journal of Enterprise Technologies* **2022**, *6(2–120)*, 85–85.
40. Pasternak, S.; Danylchenko, Y.M.; Storchak, M.; Okhrimenko, O.A. Gear Cutting with Disk-Shaped Milling Cutters. In *Advances in Gear Theory and Gear Cutting Tool Design;* Radzevich, S.P.; Storchak, M. Eds.; Springer: Cham, Switzerland, 2022; pp. 151-179.
41. Danylchenko, Y.M., Kryvosheia, A.V., Melnyk, V.Y., Tkach, P.M. Generalizing Structural Unified Model of the Synthesis of Links of Flat-Toothed Gearing Systems. In *Advances in Gear Theory and Gear Cutting Tool Design;* Radzevich, S.P.; Storchak, M. Eds.; Springer: Cham, Switzerland, 2022; pp. 445–483.
42. Neshta, A.; Kryvoruchko, D.; Hatala, M.; Ivanov, V.; Botko, F.; Radchenko, S.; Mital, D. Technological Assurance of High-Efficiency Machining of Internal Rope Threads on Computer Numerical Control Milling Machines. *J. Manuf. Sci. Eng.* **2018**, *140(7)*, 071012.
43. API SREC 7-2. Specification for Threading and Gauging of Rotary Shouldered Thread Connection. Second Edition. API: Washington, DC, USA, 2020.
44. Sandvik Coromant. Tread turning tools. Available online: https://www.sandvik.coromant.com/en-us/tools/threading-tools/thread-turning-tools (accessed on 11 March 2024).
45. Costa, C.E.; Polli, M.L. Effects of the infeed method on thread turning of AISI 304L stainless steel. *J Braz. Soc. Mech. Sci. Eng.* **2021**, *43*, 253.
46. Günay M. Investigation of the Effects on Screw Thread of Infeed Angle during External Threading. *Gazi University Journal of Science* **2011**, *24(1)*, 153-160.
47. An, Q. L.; Guo, G. G.; Zheng, X. H.; Chen, M.; Liu, G.; Zhang, Y. S. Experimental Study on Cutting Characteristics for Buttress Thread Turning of 13%Cr Stainless Steel. *Key Engineering Materials* **2010**, *443*, 262–267.
48. Onysko, O.; Kopei, V.; Kusyi, Y.; Pituley, L.; Taras, I. Tool Wear in the Process of Drill-String Connector Thread Lathe Machining. In *Lecture Notes in Networks and Systems*, New Technologies, Development and Application VI. NT 2023; Karabegovic, I., Kovačević, A., Mandzuka, S. Eds.; Springer: Cham, Switzerland, 2023; Volume 687, pp. 98–111.
49. Medvid, I.; Onysko, O.; Panchuk, V.; Pituley, L.; Schuliar, I. Kinematics of the Tapered Thread Machining by Lathe: Analytical Study. In *Lecture Notes in Mechanical Engineering*, Advanced Manufacturing Processes II. InterPartner 2020; Tonkonogyi, V., et al. Eds.; Springer: Cham, Switzerland, 2021; pp. 555–565.

 doi:10.20944/preprints202403.0719.v1

50. Onysko, O.; Panchuk, V.; Kopei, V.; Havryliv, Y.; Schuliar, I. Investigation of the influence of the cutter-tool rake angle on the accuracy of the conical helix in the tapered thread machining. *J. Phys.: Conf. Ser.* **2021,** *1781.* 012028.
51. Slătineanu, L.; Radovanovic, M.; Coteaţă, M.; Beşliu, I.; Dodun, O.; Coman, I.; Olaru, S-C. Requirements in designing a device for experimental investigation of threading accuracy**.** *MATEC Web of Conferences* **2017**, *112*, 01005.
52. Boral, P.; Gołębski, R. Technology of Manufacturing of ZC Cylindrical Worm. *Materials* 2022, *15(18)*, 6412.
53. Andrianto, M.; Wu, YR.; Arifin, A. Mathematical modeling on a novel manufacturing method for roller-gear cams using a whirl-machining process. *Int J Adv Manuf Technol* **2023**, *125*, 5015–5029.
54. Onysko, O.; Panchuk, V.; Kopei, V.; Pituley, L.; Lukan, T. Influence of Back Rake Angle of a Threading Cutter on the Drill-String Tool-Joint Pitch Diameter. In *Lecture Notes in Mechanical Engineering*, Grabchenko's international conference on Advanced manufacturing Processes. «InterPartner» 2022; Tonkonogyi V. at al. Eds.; Springer: Cham, Switzerland, 2023; pp. 200-210.
55. Onysko, O.; Medvid, I.; Panchuk, V.; Rodic, V.; Barz, C. Geometric Modeling of Lathe Cutters for Turning High-Precision Stainless Steel Tapered Threads. In *Lecture Notes in Mechanical Engineering*, Advances in Design, Simulation and Manufacturing IV. DSMIE 2021; Ivanov, V.; Trojanowska, J.; Pavlenko, I.; Zajac, J.; Peraković, D. Eds. Springer: Cham, Switzerland, 2021; pp. 472–480.
56. Kacalak, W.; Majewski, M.; Budniak, Z.; Ponomarenkow, J. Worm Gear Drives with Improved Kinematic Accuracy. *Materials* **2021**, *14*, 7825.
57. Onysko, O.; Kopei, V.; Kusyj, Y.; Kornuta, O.; Schuliar, I. Turning of NC10 Threads for Drill Pipes: Theoretical Study of the Designed Profile. In *Lecture Notes in Mechanical Engineering*, Advances in Design, Simulation and Manufacturing VI. DSMIE 2023; Ivanov, V.; Trojanowska, J.; Pavlenko, I.; Rauch, E.; Piteľ, J. Eds. Springer: Cham, Switzerland, 2023; pp. 356–366.
58. Fromentin, G.; Poulachon, G. Geometrical analysis of thread milling—part 1: evaluation of tool angles. *Int J Adv Manuf Technol* **2010**, *49*, 73–80.
59. Fu, X.; Li, K.; Li, Z. et al. A SVM-based design method for cutting edge profile stability of large-pitch thread turning tool considering vibration. *Int J Adv Manuf Technol* **2023**, *125*, 4529–4547.
60. Kacalak, W.; Szafraniec, F. Analiza kształtu i położenia strefy obróbki w procesie szlifowania powierzchni śrubowych ślimaków stożkowych. *Mechanik* **2015**, *8–9*, 159–163.